

**EMBRY-RIDDLE**  
Aeronautical University™  
SCHOLARLY COMMONS

---

Dissertations and Theses

---

12-2018

## Nonlinear Sliding Mode Observer Applied to Microalgae Growth

Rebecca J. Griffith

Follow this and additional works at: <https://commons.erau.edu/edt>



Part of the [Biological and Chemical Physics Commons](#), and the [Engineering Physics Commons](#)

---

### Scholarly Commons Citation

Griffith, Rebecca J., "Nonlinear Sliding Mode Observer Applied to Microalgae Growth" (2018).  
*Dissertations and Theses*. 432.  
<https://commons.erau.edu/edt/432>

This Thesis - Open Access is brought to you for free and open access by Scholarly Commons. It has been accepted for inclusion in Dissertations and Theses by an authorized administrator of Scholarly Commons. For more information, please contact [commons@erau.edu](mailto:commons@erau.edu).

NONLINEAR SLIDING MODE OBSERVER APPLIED TO  
MICROALGAE GROWTH

BY  
REBECCA J. GRIFFITH

A Thesis

Submitted to the Department of Physical Sciences  
and the Committee on Graduate Studies  
In partial fulfillment of the requirements  
for the degree of  
Master in Science in Engineering Physics

12/2018

Embry-Riddle Aeronautical University  
Daytona Beach, Florida

© Copyright by Rebecca J. Griffith 2018  
All Rights Reserved

NONLINEAR SLIDING MODE OBSERVER APPLIED TO  
MICROALGAE GROWTH

by

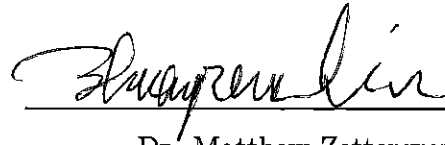
Rebecca J. Griffith

This thesis was prepared under the direction of the candidate's Thesis Committee with Co-Chairs, Dr. Sergey Drakunov, Professor of Engineering Physics and Dr. Karen Gaines, Dean of College of Arts and Sciences, Daytona Beach Campus and Thesis Committee Member, Dr. William MacKunis, Associate Professor of Engineering Physics, Daytona Beach Campus, and has been approved by the Thesis Committee. It was submitted to the Department of Physical Sciences in partial fulfillment of the requirements of the degree of Master of Science in Engineering Physics

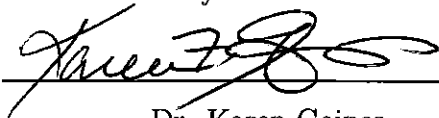
THESIS COMMITTEE:



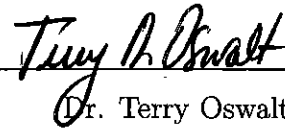
Dr. Sergey Drakunov,  
Committee Co-Chair,  
Physical Sciences



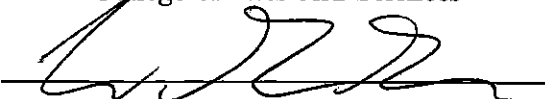
Dr. Matthew Zettergren,  
Graduate Program Chair, Engineering Physics



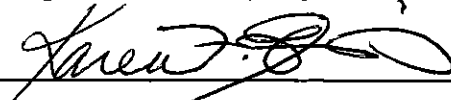
Dr. Karen Gaines,  
Committee Co-Chair,  
College of Arts and Sciences



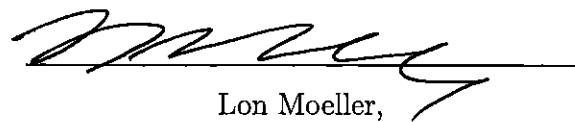
Dr. Terry Oswalt,  
Department Chair, Physical Sciences



Dr. William MacKunis,  
Committee Member,  
Physical Sciences



Dr. Karen Gaines,  
Dean, College of Arts and Sciences



Lon Moeller,  
Senior V.P. for Academic Affairs and Provost

# Abstract

Modeling biological processes, such as algae growth, is an area of ongoing research. The ability to understand the multitude of parameters that influence this system provides a platform for better understanding the dynamics of microalgae growth. Empirical modeling efforts look to understand sources of driving nutrients that influence harmful algal blooms (HABs). These harmful algal blooms are dense aggregates that have an increasingly negative impact on local economics, marine and freshwater systems, and public health. They result from a high influx of nitrogen and nutrients that drive the algae biomass to exponentially grow. This growth blocks out the sun, potentially releases dangerous toxins, and suffocates marine life, damaging ecosystems, especially in Florida.

Modeling microalgae behavior and growth is complex due to its nonlinear behavior and coupled variables. Recently, cultivating oleaginous microalgae for biofuel production has been another region of ongoing research, especially application of observer theory to estimate internal parameters that are not easily measured in algal systems. Linear observer theory has generally been applied to algae growth systems to estimate internal parameters that are beyond hardware sensor capabilities, but they are still severely limited. Nonlinear observer theory application to biological systems is still relatively new. This thesis explores the application of a nonlinear observer based off sliding mode to an algae system. Sliding mode is derived from modern control theory and is based off variable structure control. An algae system is modeled using the widely accepted Droop model for algae growth and a linear and nonlinear sliding mode observer is developed for the system to estimate internal nitrogen within the algae biomass.

# Acknowledgments

I would like to thank Dr. Sergey Drakunov and Dr. Karen Gaines for providing me with this opportunity and for their mentorship, expertise, and enthusiasm towards this unique project and completion of this thesis. Thank you to the NASA Florida Space Grant Consortium with the Master's Fellowship during the 2017-2018 year for granting me the opportunity to continue pursuing this thesis.

# Contents

<b>Abstract</b>	<b>iv</b>
<b>Acknowledgments</b>	<b>v</b>
<b>1 Introduction</b>	<b>1</b>
1.1 Modeling Biological Systems . . . . .	1
1.1.1 Empirical Modeling . . . . .	1
1.1.2 Numerical Modeling . . . . .	5
1.2 Modeling Microbiological Processes . . . . .	7
1.2.1 Monod Model . . . . .	7
1.2.2 Nitrogen Fixation . . . . .	10
1.3 Parameters and State Estimations . . . . .	13
1.4 Motivation and General Problem Statement . . . . .	14
<b>2 Mathematical Methods</b>	<b>15</b>
2.1 Model Discussion . . . . .	15
2.2 Results From Theory of Dynamical Systems . . . . .	19
2.2.1 Stability and Equilibrium . . . . .	19
2.2.2 Stability of an Equilibrium . . . . .	19
2.2.3 Linearization of the Algae Growth Model System . . . . .	23
2.2.4 Sliding Mode Phenomenon in Dynamical Systems . . . . .	24
2.3 Linear System Observer Theory . . . . .	28
2.3.1 System Observability . . . . .	28
2.3.2 Linear State Observers . . . . .	29

2.3.3	Kalman-Bucy Filter . . . . .	31
2.3.4	Sliding Mode Observer for Linear System . . . . .	32
2.4	Nonlinear Observer Theory . . . . .	33
2.4.1	Extended Kalman Filter . . . . .	34
2.4.2	Nonlinear Sliding Mode Observer . . . . .	35
2.4.3	Problem Setup . . . . .	37
<b>3</b>	<b>Results</b>	<b>39</b>
3.1	Simplified Droop Model Results . . . . .	39
3.2	State Observers Applied to Microalgae System . . . . .	44
3.2.1	Linear State Observer . . . . .	45
3.2.2	Nonlinear Sliding Mode Observer . . . . .	49
3.3	Other Analysis . . . . .	52
<b>4</b>	<b>Conclusion and Discussion</b>	<b>54</b>
4.1	Future Work . . . . .	55
4.1.1	Improve Model . . . . .	55
4.2	Implications of Research . . . . .	56
<b>A</b>	<b>Parameters Used for Algal Growth Simulation</b>	<b>58</b>
<b>B</b>	<b>MATLAB Code</b>	<b>59</b>



# List of Tables

A.1 Parameter values used for model . . . . . 58

# List of Figures

1.1	Mississippi Watershed River System [48] . . . . .	3
1.2	Red Tide off the Florida Gulf Coast on August 24, 2018 [51] . . . . .	9
1.3	Annual Total Nitrogen Loads in the Mississippi/Atchafalaya River Basin Transported to the Gulf of Mexico from 1980-2015 [1] . . . . .	11
1.4	Demonstration of a state observer applied to a system. [33] . . . . .	14
2.1	Equilibrium of System With a Small Disturbance . . . . .	22
2.2	State trajectories for $\hat{x} = -sign(x)$ [17] . . . . .	25
2.3	Sliding mode control for an on and off control system [33] . . . . .	27
2.4	Block diagram of a Luenberger Observer[7] [33] . . . . .	30
2.5	Block Diagram of a Linear Sliding Mode Observer . . . . .	33
3.1	Algae growth demonstrated by Droop's Model . . . . .	40
3.2	Internal nitrogen growth closely follows algae biomass growth . . . . .	41
3.3	External nitrates ( $NO_3^-$ ) decrease when consumed by microalgae . . . . .	42
3.4	Algae biomass concentrations are more representative to nature . . . . .	43
3.5	Internal Nitrogen . . . . .	43
3.6	External Nitrate . . . . .	44
3.7	Linear State Observer for Biomass . . . . .	45
3.8	Linear State Observer for Internal Nitrogen . . . . .	46
3.9	Linear State Observer for Internal Nitrogen Showing Convergence . . . . .	47
3.10	Linear State Observer for External Nutrients . . . . .	48
3.11	Sliding Mode Observer applied to internal nitrogen . . . . .	52

3.12 Monte Carlo simulation showing a distribution of biological model based off random inputs into the system. . . . .	53
--	----

# Chapter 1

## Introduction

### 1.1 Modeling Biological Systems

Modeling biological systems is extremely dynamic and complex. Researchers look to develop both empirical and numerical methods to describe biological systems and events in order to understand the reason a system functions in a particular manner. The layout for this chapter includes a discussion on empirical modeling efforts of biological systems in aquatic environments, with a focus on nutrient origins. Following this, the second subsection of this chapter looks at numerical models for biological systems with first discussing large scale predator-prey systems and then moving to discuss models for microbiological systems focusing on algal systems. This chapter then concludes with a brief discussion of general observer theory and a discussion for the motivation of this thesis.

#### 1.1.1 Empirical Modeling

Empirical modeling of biological systems in aquatic environments, especially along the coast, strongly depends on understanding where nutrients originate and how they are transported. Empirical models depend on relentless sample taking over a wide surface area thereby making studies extremely challenging and time consuming. For example, ecological modeling in applications for risk assessment work to understand

current ecosystem patterns, processes and functions in order to predict future conditions. Spatially explicit models are used and in order to predict future conditions, ecosystem modelers need to take different scales of ecological organizations and its complexity into account. The protocols need to be designed to consider the host of parameters specific to that ecosystem [26].

Riverine and coastal eutrophication from natural and human derived nutrients such as carbon, nitrogen, and phosphorus, among others, have a major impact on biological systems located in the Gulf of Mexico[31]. Modeling nutrient transport and the effects it has on the Gulf's biological systems is a major source of research due to the current Red Tide that is plaguing the Gulf. Empirical modeling efforts focus primarily on nutrient loads, which reflect the rate of the delivery of nutrients from water and/or air sheds[27].

### **Watershed Modeling**

Watersheds are regions where the water from all nearby land area drains into one stream, lake, or river that it surrounds. The Mississippi River watershed is the largest watershed in the United States where all the water collected along the watershed will flow into the Gulf of Mexico which can be seen in Figure 1.1



Figure 1.1: Mississippi Watershed River System [48]

This watershed collects all the nutrients, including bioactive nitrogen, from the Plains which will flow into the Gulf of Mexico making the Gulf extremely prone to biological events such as algal blooms[2].

Changes such as an increase in agricultural production and energy consumption have resulted in massive mobilization of bioactive nutrients such as nitrogen, phosphorus, and carbon in the global hydrological cycle. With the increase of fertilizer use, the rate of biologically active nitrogen that enters into the global watershed has increased[46]. Modeling efforts focus on developing relationships between nutrient loading sources into the watershed around the U.S and nutrient outputs into the Gulf. SPARROW is one model(discussed below) that is used by the EPA and other research efforts in conjunction with other local models to develop correlations between nutrient sources and their final destination[27].

## SPARROW

A popular empirical model, SPARROW (Spatially Referenced Regressions On Watershed attributes) estimates the amount of a contaminant that is transported from an inland watershed to larger bodies of water by combining monitoring data with information on watershed characteristics and sources of contaminants. SPARROW uses a statistically estimated nonlinear regression relationship to describe spatially referenced watershed and channel characteristics as known as predictors to instream loads(response)[45]. The equations in SPARROW describe the average rate of movement of material, such as nutrients, through watersheds from sources on land to stream channels, then downstream through these various stream channels. SPARROW can predict long-term mean annual instream nitrogen loads as a function of nitrogen sources, nitrogen attenuation on the landscape, and nitrogen losses that occur within the streams shown as

$$L_{instream} = L_{catchment_i} + L_{upstream_i} \quad (1.1)$$

Where the load at downstream node  $i$  is denoted as  $L_{instream}$ , the original load within the catchment  $i$  is  $L_{catchment}$ , and  $L_{upstgream}$  is the generated load within the catchments for upstream reaches and is transported to the downstream node of each  $i$  by use of the stream network[31]. SPARROW can be used to describe water quality conditions, identify sources of nutrients/containments, simulate alternative conditions, as well as assist with research efforts.

### Nutrient Impact on Water Quality

Using large-scale modeling efforts such as SPARROW, the EPA establishes water quality standards that provide recommendations to states, tribes, and territories in order to maintain their local water systems. These standards attempt to look at all possible chemicals, nutrients, and pollutants that can enter the water systems and establish allowable limits. The two most closely monitored nutrients in the state of Florida are Total Nitrogen (TN) and Total Phosphorus (TP) and depending on the water type and location, these limits will vary. They are calculated as Annual

Geometric Means (AGM) that cannot be exceeded more than once in a three year period. The lowest TN limit is in the Upper Keys as 0.18mg/L of nitrogen with the highest limit in the West/Central river systems of 1.65mg/L with samples collected monthly[3].

## 1.1.2 Numerical Modeling

### Predator-Prey Models

Species in a biological system will compete for resources, evolve and/or disperse for the survival of the species and what influences that objective. These systems are usually described by predator-prey models where they usually display loss-win interactions [14] Take two populations with reference to time,  $t$ , described by  $x(t)$  and  $y(t)$  where  $x$  and  $y$  represent prey and predator population numbers respectively. A general predator-prey model takes the time derivatives of  $x(t)$  and  $y(t)$  respectively and a model of interacting populations is described by two autonomous differential equations,

$$\dot{x} = f(x, y) \tag{1.2}$$

$$\dot{y} = g(x, y) \tag{1.3}$$

where  $f(x, y)$  and  $g(x, y)$  are respective per capita growth rates for the two species.

### Lotka-Volterra

One of the earliest models in mathematical ecology is the Lotka-Volterra model illustrating one of the simplest forms of predator-prey interactions based on a linear per-capita growth rate.

$$\frac{\dot{x}}{x} = b - py \tag{1.4}$$



$$\frac{\dot{y}}{y} = rx - d \quad (1.5)$$

Where  $b$  denotes the growth rate of species  $x$ , prey, in the absence of interaction with the predator,  $y$ . The impact of predation on  $\frac{\dot{x}}{x}$  is described by  $p$ , and  $d$  is the removal rate by either death or emigration of the predator without interaction with the prey. The net growth of the predator population in response to the size of the available prey population is described by  $rx$ , giving the model to be [47]

$$\dot{x} = (b - py)x \quad (1.6)$$

$$\dot{y} = (rx - d)y \quad (1.7)$$

This model was independently derived by Alfred James Lotka and Vito Volterra in 1925 and 1926, respectively [14].

### Kolmogorov Equations

Kolmogorov generalized Lotka-Volterra where instead of a first approximation of real rates of increase, he considered the most general case possible

$$\dot{x} = S(x, y) \quad \dot{y} = W(x, y) \quad (1.8)$$

and developed a postulate stating that if the rate increases  $S$  and  $W$  are continuously differentiable, basic conditions can be applied which will provide a more realistic predator-prey interaction description [47]. Kolmogorov presents a set of conditions

$$\frac{\partial S}{\partial y} < 0, \quad \frac{\partial W}{\partial y} < 0 \quad (1.9)$$

where the second does not satisfy Lotka-Volterra and a third condition

$$W(K, 0) > 0 \quad (1.10)$$

where the equilibrium,  $(K, 0)$ , is only composed of prey, not predators which will

imply that there is at least one equilibrium with coexistence of both the predator and prey species[47]. Kolmogorov also noticed that his conditions become invalid once the prey population density becomes extremely small, also known as the "Allee Effect" where the rate of increase, for example of a prey population, can decrease and become negative if the density of the population is too small [47].

## 1.2 Modeling Microbiological Processes

### 1.2.1 Monod Model

Another approach discussing predator-prey interaction looks at microorganisms such as bacteria that take in nutrients. The Monod Model is a mathematical model for growth of microorganisms named after Jacques Monod who proposed using an equation to relate microbial growth rates in an aqueous environment to the concentration of a limiting nutrient. These organisms are influenced by a limited uptake rate and the Jacob-Monod model looks at the kinetic growth of microorganisms under a substrate limited condition shown below [20].

$$\frac{ds}{dt} = \frac{-ksx}{k_s + s} \quad (1.11)$$

$$\frac{dx}{dt} = y \frac{ksx}{k_s + s} - bx \quad (1.12)$$

where,  $s$  is the growth limiting substrate concentration,  $x$  is the biomass concentration,  $k$  is the maximum specific uptake rate of the substrate,  $k_s$  is the half saturation constant for growth,  $y$  is the yield coefficient, and  $b$  is the decay coefficient [20].

Unlike large scale predator-prey models, the Monod model[41] illustrates kinetics of growth of micro-organisms under that substrate limited condition. This was quantitatively defined by Monod in 1949. The Monod kinetic model has a wide application to wastewater treatment, bioremediation, as well as other various applications to environmental modeling[20].

## Algae Systems

Algae are simple photosynthetic aquatic organisms that have many types of life cycles. They can range from microscopic (microalgae), to larger seaweeds (macroalgae) such as giant kelp that live off the coast of California [43]. Unlike other plants, microalgae do not have roots, stems, or leaves. They adapt well to their environment. Algal diversity and abundance vary based on environment. As terrestrial plant abundance and diversity primarily depend upon temperature and precipitation, aquatic plants such as algae are influenced primarily by light and nutrients. When there is an abundance of nutrients in the water, algal cell numbers will become great enough to produce visible patches called "blooms"[42] which can have adverse effects on local ecological systems.

## Modeling Algae Growth

Since algae only need sunlight, water, carbon dioxide, and some inorganic nutrients, algal biomass can grow very quickly and modeling this growth can be extremely complex. Understanding how algae grow is essential to pursue the use of this taxa in biofuel production, food production and supplementation as well as to try to prevent Harmful Algal Blooms (HAB).

Autotrophic microalgae and cyanobacteria use photons as an energy source to fix carbon dioxide. These microorganisms have recently received specific attention in the framework of renewable energy[9]. Microalgae have a high photosynthetic yield compared to terrestrial plants and this leads to a potentially large algal biomass production [16]. After the biomass is nitrogen starved, it can reach a very high lipid content which can be converted into biofuel [9].

## Harmful Algal Blooms

Harmful Algal Bloom, also known as HABs, are characterized by the proliferation and occasional dominance of an algal species in an ecosystem. These microalgal species

increase in abundance until their pigments color the water and change its natural state. HABs can either be toxic or nontoxic depending upon if the microalgae species releases any toxins. Non-toxic HAB species can cause damage to ecosystems because of the sheer biomass that is formed during a bloom; which can cause oxygen depletion, an alteration in the local habitat, and potential displacement of local aquatic life. Algae can enter gills of fish and other invertebrates and smother corals as well as other submerged vegetation. Toxic HABs have an adverse affect on both marine ecosystems and human life. Toxins can cause illness and death to humans, birds and other sea life through a transfer of toxins in the food web [5].



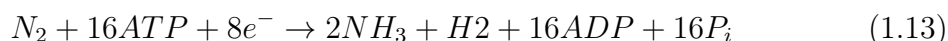
Figure 1.2: Red Tide off the Florida Gulf Coast on August 24, 2018 [51]

Recently, Florida has been plagued by HABs in the Gulf of Mexico in the form of what is commonly known as "Red Tide" shown in Figure 1.2 which is caused by a species of microalgae called *Karenia brevis* that persists along the South Gulf Coast of Florida. The primary cause of algal blooms comes from nutrient pollution. Primary nutrients that drive growth are nitrogen and phosphorus and have the capability to push algae toward unrestrained growth. It is important to understand where these driving nutrients originate.

## 1.2.2 Nitrogen Fixation

### Natural Nitrogen Fixation

Nitrogen Fixation is a naturally occurring process and is essential for some forms of life because inorganic nitrogen compounds are required for biosynthesis of plants and other life forms. This process involves taking nitrogen in the Earth's atmosphere in the form of  $N_2$  and converts it into ammonia ( $NH_3$ ) or other molecules that can be consumed by living organisms [34]. This fixation frees nitrogen atoms from their triply bonded diatom form  $N \equiv N$  and then allows them to be used in multiple ways. Nitrogen can be fix biologically or non-biologically. Non-biological nitrogen fixation occurs when lightning in the air converts atmospheric nitrogen and oxygen into nitrogen oxides  $NO_x$  where these nitrogen oxides can react with water to make various acids such as nitric acid or nitrous acid that will seep into the soil to make nitrate which is then consumed by plants[30]. Biological nitrogen fixation was discovered by Hermann Hellriegel and Martinus Beijerinck and occurs when atmospheric nitrogen is converted into ammonia by nitrogenase (metallo)enzymes giving the overall reaction



ATP is the organic chemical adenosine triphosphate which provides energy to drive cellular processes where energy is used and the product adenosine diphosphate is formed. One process is nitrogen fixation. There are certain microorganisms that fix nitrogen, such as legumes and diazotrophs as well as cyanobacteria. Cyanobacteria under the domain of diazotrophs inhabit almost all illuminated environments on Earth and play a vital role in fixing nitrogen as part of the nitrogen cycle. They are primarily responsible for naturally introducing nitrogen into biological systems [8].

### Synthetic Nitrogen Fixation

Nitrogen fixation naturally occurs due to the nitrogen cycle described in the above sub-section. However, nitrogen entry into the ecosystem has exponentially increased post-World War II due to using nitrogen and phosphorus fertilizer for agriculture.

The increase in human population causes an increase in the demands for food and energy, which drives the need to synthetically fix nitrogen for plant growth. This has dramatically increased the rate of nutrient export to coastal waters via watersheds [27]. The Mississippi Watershed Basin Figure 1.1 encompasses a lot of farmland in the United States, causing nitrogen rich fertilizer to drain into the watershed and flow to the Mississippi River and into the Gulf Coast[1]. The excessive nutrient loads trigger an overgrowth of algae that lead to blooms in the Gulf of Mexico.

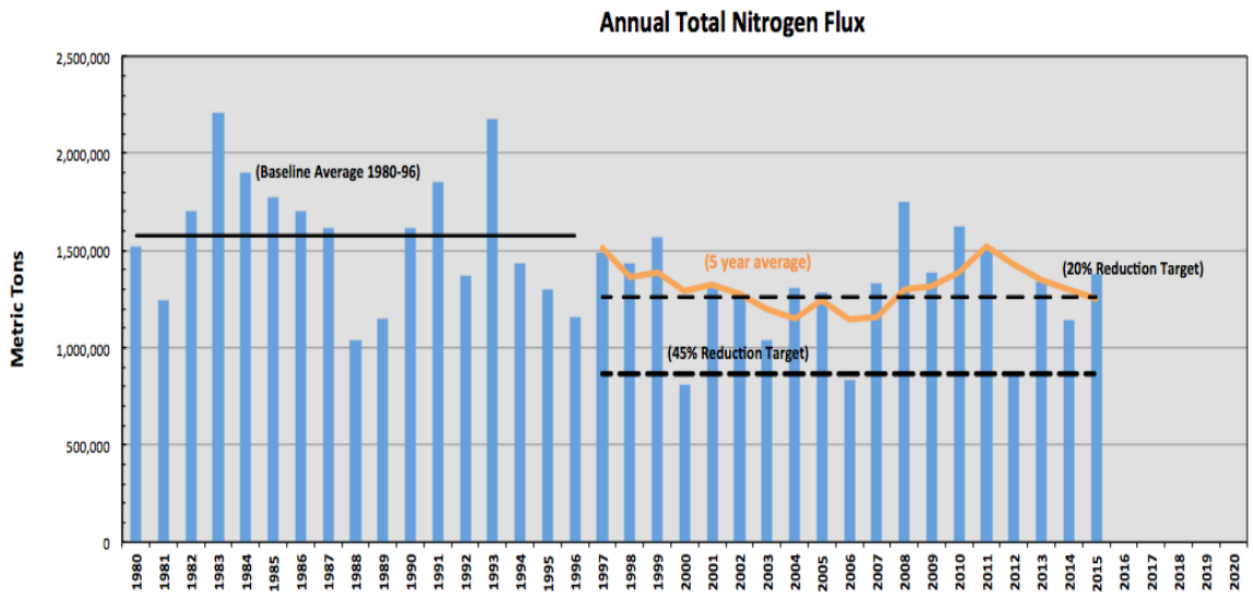


Figure 1.3: Annual Total Nitrogen Loads in the Mississippi/Atchafalaya River Basin Transported to the Gulf of Mexico from 1980-2015 [1]

The EPA monitors nitrogen loads which is presented in Figure 1.3. Average Total Nitrogen loads range from a high of 2,200,00 metric tons of nitrogen in 1983 and has been on a decreasing trend where annual nitrogen load averages fall to about 1,300,000 metric tons in 2015. Models such as SPARROW and others used from the USGS and Texas A & M University have assisted the EPA to determine total nutrient loads [1], specifically nitrogen and help establish water quality standards.

### Biofuel Production

Biofuels from microalgae show a promising area of research. Understanding their growth and applying numerical models to determine the change in a growing system will allow for an efficient method to determine the performance of newer biofuels. Microalgae show a promising source of biomass for sustainable energy production. This photosynthetic microorganism can accumulate a large amount of neutral lipids used in biodiesel production, as well as carbohydrates. The driving environmental conditions such as the availability of light and nutrients such as nitrogen influence microalgal growth as well as its biochemical composition[38]. The process for converting algal biomass into fuel is simply put: the algae is grown, harvested, dewatered then the oil is extracted so the lipids can be converted to biodiesel while the remaining algae is fermented and converted into bioethanol.

### Droop Model

The Monod kinetic model demonstrates microorganism growth and decay with regards to introducing the limited uptake rate. Microalgae growth does not follow this trend. Microalgae are known for their ability to uncouple the uptake of nutrients, such as inorganic nitrogen, phosphorus, micronutrients, etc., from growth. Meaning, the classic Monod model where nutrient uptake and growth are proportional, can no longer be applied [9].

The Droop model writes

$$\dot{s} = Ds_{in} - \rho(s)x - Ds \quad (1.14)$$

$$\dot{q} = \rho(s) - \mu(q)q \quad (1.15)$$

$$\dot{x} = \mu(q)x - Dx \quad (1.16)$$

where  $s$  is the limiting dissolved inorganic nitrogen in the form of nitrate or ammonia,  $q$  is the internal nitrogen cell quota, and  $x$  is the biomass which is related to the

internal concentration of the limiting element[9]. The growth rate  $\mu$  of the algal biomass  $x$  is coupled to the internal concentration of the limiting nutrient. Droop introduces his internal nitrogen cell quota  $q$  which is a function of the amount of nitrogen per biomass unit [23]. The absorption rate,  $\rho(s)$ , is described by Michael-Menten kinetics [9], [15] shown

$$\rho(s) = \rho_m \frac{s}{x + K_s} \quad (1.17)$$

and  $s$  is the limiting dissolved inorganic nitrogen,  $K_s$  is the half saturation constant for the substrate uptake and the maximum uptake rate is denoted as  $\rho_m$ . The growth rate based on the Droop function

$$\mu(q) = \tilde{\mu} \left(1 - \frac{Q_o}{q}\right) \quad (1.18)$$

where  $\tilde{\mu}$  is the growth rate at hypothetical infinite quota, while the minimal cell quota is denoted as  $Q_o$ . The Droop model demonstrates that for a consistent initial condition, the internal quota will stay larger than the minimal cell quota therefore allowing the growth rate to always stay positive[9],[50].

### 1.3 Parameters and State Estimations

A primary limitation for estimating parameters and monitoring systems is due to the difficulty of measuring all components of the model that include its states and parameters. Very few sensors exist that are reliable and affordable and can be used to take measurements in real time to obtain desired values for difficult to measure parameters. Other methods are extremely difficult and their complicated and sophisticated operations normally do not outweigh the need to use them for obtaining measurements. In control theory, there is a method for state estimation which is known as observers. Observers can be built instead to obtain estimations of desired measurements based off inputs and outputs of the system.



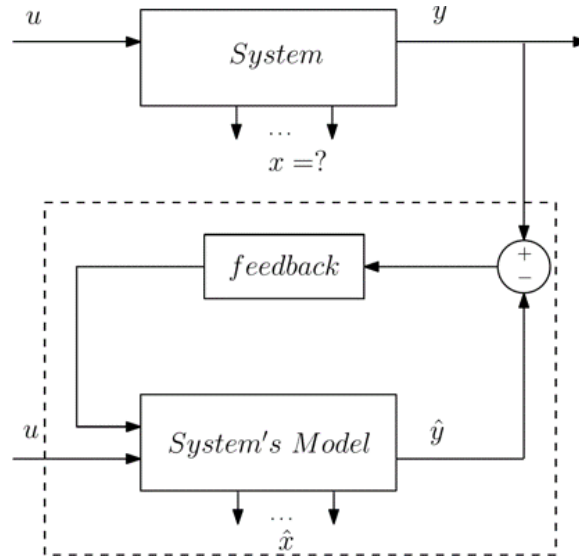


Figure 1.4: Demonstration of a state observer applied to a system. [33]

This state vector feedback design offers advantages in regards to system performance and analysis. Unfortunately, the disadvantage in this system is the system state vector is not readily available for direct measurement. Therefore, the control function cannot be evaluated and either the control scheme for the system will have to be abandoned or a substitute state vector needs to be found. State observer technique is derived from control theory and is an algorithm for estimating the states of the system when only some outputs and inputs are available [20] illustrated in Figure 1.4. Observer theory is very well developed for linear systems. Basic structure consists of the system made with some additional inputs that are used to steer the output of the observer to the measured output of the estimated system [20]. After some time, the state of the real system is approximately equal to the state of the observer which will give estimates of the variable not easily measured.

## 1.4 Motivation and General Problem Statement

The goal of this thesis is to apply the general theory of observers, specifically nonlinear observer theory, to a nonlinear biological system modeled by Droop's formulation for microalgal growth in order to observe internal parameters in the system.

# Chapter 2

## Mathematical Methods

This chapter will go into a detailed discussion of the model used as well as provide a more specific discussion of linear observer theory and nonlinear observer theory. The linear stability, nonlinear stability and observability of the system are explored. This chapter then concludes with a detailed discussion on the three observers used for the model.

### 2.1 Model Discussion

#### Original Model

The original model in Equations 2.1, 2.2, and 2.3 from [10] demonstrate growth of an algal biomass using a nutrient concentration under the nitrate form  $NO_3^-$ . In order to couple the nutrient uptake rate  $\lambda$  and the growth rate  $\mu$ , Droop introduced a cell quota  $q(t, x)$  which is defined as the amount of internal nutrients per biomass unit:  $q = \frac{C^2}{C^1}$ . As a result, the following three nonlinear coupled equations are presented below [10]:

$$\frac{\partial \rho C^1}{\partial t} + \frac{\partial \rho u C^1}{\partial x} + \frac{\partial \rho w C^1}{\partial z} = \mu_{C^1} \left( \frac{\partial^2 C^1}{\partial x^2} + \frac{\partial^2 C^1}{\partial z^2} \right) + \rho(\mu(q, I)C^1 - RC^1) \quad (2.1)$$

$$\frac{\partial \rho C^2}{\partial t} + \frac{\partial \rho u C^2}{\partial x} + \frac{\partial \rho w C^2}{\partial z} = \mu_{C^2} \left( \frac{\partial^2 C^2}{\partial x^2} + \frac{\partial^2 C^2}{\partial z^2} \right) + \rho(\lambda(C^3, q)C^1 - RC^2) \quad (2.2)$$

$$\frac{\partial \rho C^3}{\partial t} + \frac{\partial \rho u C^3}{\partial x} + \frac{\partial \rho w C^3}{\partial z} = \mu_{C^3} \left( \frac{\partial^2 C^3}{\partial x^2} + \frac{\partial^2 C^3}{\partial z^2} \right) - \rho(\lambda(C^3, q))C^1 \quad (2.3)$$

where  $C^1$  is the algal biomass ( $gCm^{-3}$ ),  $C^2$  is nitrogen concentration contained in the algal biomass ( $gNm^{-3}$ ), and  $C^3$  is nutrient concentration ( $gNm^{-3}$ ) [10].  $R$  is a constant loss factor representing the daily respiration and mortality of the biomass. The intra-cellular quota is

$$\mu(q) = \bar{\mu} \left( 1 - \frac{Q_o}{q} \right) \quad (2.4)$$

and the hypothetical growth rate is defined as  $\bar{\mu}$ , and  $Q_o$  is the minimum internal quota that is required for growth.

The nitrate uptake rate,  $\lambda(C^3)$  is a function of external nitrate [10][40]

$$\lambda(C^3) = \bar{\lambda} \frac{C^3}{C^3 + K_3} \quad (2.5)$$

where the half saturation constant is denoted as  $K_3$  and  $\bar{\lambda}$  is the maximum uptake rate.

Light intensity,  $I$ , is computed

$$I(z) = I_o e^{-\psi(C^2, I^*, z)} \quad (2.6)$$

where

$$\psi(C^2, I^*, z) = \int_0^z (a\gamma(I^*)C^2(z) + b) dz \quad (2.7)$$

with  $I^*$  being the average (space and time) light in the water column the day before and  $I_o$  is the light intensity hitting the water's surface. It is assumed that  $I_o$  is periodic

with a fundamental period being one day.

$$I_o = I_o^{max}(0, \sin(2\pi t)) \quad (2.8)$$

When light is incorporated into the algae growth model for this thesis, it is assumed light is hitting the algae on the surface of the water and it is periodic and will follow Equation 2.8.

Equations 2.1, 2.7, and 2.8 modeled from [44] can expand the growth rate to now take into account light intensity

$$\mu(q, I) = \tilde{\mu} \frac{I}{I + K_{sI} + \frac{I^2}{K_{iI}}} \left(1 - \frac{Q_o}{q}\right) \quad (2.9)$$

where  $\tilde{\mu}, K_{sI}, K_{iI}$  are three given constants [10]

In order to avoid infinite substrate ( $NO_3$ ) uptake in the dark a down regulation of the internal quota of the uptake rate is included which is described below [10]

$$\lambda(C^3, q) = \bar{\lambda} \frac{C^3}{C^3 + K_3} \left(1 - \frac{q}{Q_l}\right) \quad (2.10)$$

where the maximum achievable quota in the system is denoted as  $Q_l$ .

This model includes advection and diffusion terms denoted as the second order derivatives in the three main equations with the corresponding diffusion coefficients ( $\mu_{C^1}, \mu_{C^2}, \mu_{C^3}$ ) and fluid velocities ( $u, w$ ) along the  $x$  and  $z$  direction [10].

This complex biological model is coupled with a 2D hydrodynamic model representing free surface fluid flow that is set into motion by a paddlewheel.

### Simplifications and Assumptions to the Original Model

It is first assumed the system is non-translating and diffusing, where the terms  $\frac{\partial \rho u C^1}{\partial x} + \frac{\partial \rho w C^1}{\partial z}$ ,  $\frac{\partial \rho u C^1}{\partial x} + \frac{\partial \rho w C^2}{\partial z}$ , and  $\frac{\partial \rho u C^3}{\partial x} + \frac{\partial \rho w C^3}{\partial z}$  on the left-hand side are set to zero and the second order partial derivatives  $\frac{\partial^2 C^1}{\partial x^2} + \frac{\partial^2 C^1}{\partial z^2}$ ,  $\frac{\partial^2 C^2}{\partial x^2} + \frac{\partial^2 C^2}{\partial z^2}$ , and  $\frac{\partial^2 C^3}{\partial x^2} + \frac{\partial^2 C^3}{\partial z^2}$  on the right-hand side can also be set to zero.

The density ( $\rho$ ) is also assumed to be constant. In order to simplify the model, light intensity will be grouped into one variable  $I$  where this describes the growth of the

algae on the surface of the water and light intensity is only hitting the algae on the surface following a periodic day/night cycle.

### Simplified Model

With these assumptions the model can be simplified to a system of ODEs and then converted into state-space notation which yields the following three nonlinear coupled differential equations that describe the biological system:

$$\dot{x}_1 = \mu(q, I)x_1 - Rx_1 \quad (2.11)$$

$$\dot{x}_2 = \lambda(q, I)x_1 - Rx_2 \quad (2.12)$$

$$\dot{x}_3 = -\lambda(q, I)x_1 + N \quad (2.13)$$

where  $x_1$  is the time-rate growth of micro-algae biomass and  $x_2$  and  $x_3$  describe the time-rate growth and consumption of nitrogen and nutrient concentration respectively.

Light intensity is periodic, Equation 2.9 can be simplified into one variable,  $\gamma$ .

$$\gamma = \tilde{\mu} \frac{I}{I + K_{sI} + \frac{I^2}{K_{iI}}} \quad (2.14)$$

Combining the previous assumptions, the following simplified model 2.15, 2.16, and 2.17 is

$$\dot{x}_1 = \gamma \left( 1 - \frac{Q_o x_1}{x_2} \right) x_1 - Rx_1 \quad (2.15)$$

$$\dot{x}_2 = \bar{\lambda} \left( \frac{x_3}{x_3 + K_3} \right) \left( 1 - \frac{x_2}{Q_l x_1} \right) x_1 - Rx_2 \quad (2.16)$$

$$\dot{x}_3 = -\bar{\lambda} \left( \frac{x_3}{x_3 + K_3} \right) \left( 1 - \frac{x_2}{Q_l x_1} \right) x_1 + N \quad (2.17)$$

Where  $N$  is a control nutrient input into the system to sustain growth within the system. Parameter inputs for the system are shown in Table A.1.

## 2.2 Results From Theory of Dynamical Systems

This section will describe the necessary mathematical tools that will be used on the microalgal system.

### 2.2.1 Stability and Equilibrium

In general, an equilibrium is defined as a constant solution of a dynamical system. Specifically, for a system of ordinary differential equations where a nonlinear system of the form

$$\dot{\mathbf{x}} = \mathbf{f}(\mathbf{x}, t) \quad (2.18)$$

where  $\mathbf{x}$  is the state vector such that  $x \in R^n$ , and the equilibria  $x^*$  can be found by solving the algebraic equation so that

$$\mathbf{f}(\mathbf{x}^*, t) = 0 \quad (2.19)$$

for all of  $t$ [52].

### 2.2.2 Stability of an Equilibrium

When analyzing a nonlinear system, is important to test the system's equilibrium for stability. Currently Equations 2.15, 2.16, and 2.17 are in a nonlinear dynamic form described in 2.19 where  $x = x_1 \dots x_n^T$  is a state vector with an equilibrium point  $x^*$  where

$$f(x^*, t) = 0 \quad (2.20)$$

for all of  $t$ .

If an equilibrium point is isolated it will have *Lyapunov stability* if for any  $\epsilon > 0$  a real positive number will exist  $\delta(\epsilon, t_o)$  for all  $t \geq t_o$  which gives

$$\|x(t_o) - x^*\| \leq \delta \Rightarrow \|x(t) - x^*\| \leq \epsilon \quad (2.21)$$

where the Euclidean norm of the vector  $x$  is denoted as  $\|x\|$

$$\|x\| = \sqrt{x^T x} \quad (2.22)$$

The isolated equilibrium point is *locally asymptotically stable* if it has the previous *Lyapunov stability* and

$$\|x(t_o) - x^*\| \leq \delta \Rightarrow x(t) \rightarrow x^* \quad (2.23)$$

when  $t \rightarrow \infty$ .

The isolated equilibrium point will be *globally asymptotically stable* if it holds the above *Lyapunov stability* and demonstrates

$$x(t) \rightarrow x^* \quad (2.24)$$

for any initial condition  $x(t_o)$  as well as  $t \rightarrow \infty$ .

### Stability Analysis of Linear Systems

A linear system 2.25, will be stable about the equilibrium point  $x^* \equiv 0$  if all the eigenvalues of the matrix  $A$  have non-positive real parts and no repeated eigenvalues on the imaginary axis [52]. When a linearized system described as

$$\dot{x} = \mathbf{A}x \quad (2.25)$$

is said to be unstable if any of the eigenvalues have a positive real part or the eigenvalues are repeated [52]. This stability analysis plays an important role when the stability of a nonlinear dynamic system is considered.

### Nonlinear System Stability Analysis

There are two methods for analyzing the stability of a nonlinear system. The first is through the method of linearization. Let  $x^*$  be the equilibrium of 2.18, then introducing  $\bar{x} = x - x^*$  we can have  $\dot{\bar{x}} = f(\bar{x} + x^*, t)$ . For small  $\bar{x}$  using a Taylor series expansion of  $f$  we have

$$\dot{\bar{x}} \approx \frac{\partial f}{\partial x}(x^*, t)\bar{x} \quad (2.26)$$

or

$$\dot{\hat{x}} = A(t)\hat{x} \quad (2.27)$$

which is linearized version of the nonlinear system 2.18. Assuming that  $A(t)$  is a constant matrix we can use the linear system stability analysis to obtain stability conditions for the nonlinear system 2.18. If the linearized system is asymptotically stable then the corresponding equilibrium of the nonlinear system is also asymptotically stable. The second method is through the use of the Lyapunov function. When the nonlinear system is evaluated at  $x^*$  the system will approach zero. If in a finite neighborhood  $D$  of  $x^*$  there exists a positive-definite scale function  $E(x) > 0$ , also known as a Lyapunov function, with continuous first partial derivatives with respect to  $x$  and  $xt$ , such that its derivative is negative in  $D$ , then the equilibrium  $x^*$  is asymptotically stable. Moreover,  $\dot{E}(\mathbf{x}) \leq 0$  for all  $\mathbf{x} \neq \mathbf{x}^*$  for all  $t$ . If  $\dot{E}(\mathbf{x}) > 0$  for all  $\mathbf{x} \neq \mathbf{x}^*$  then the equilibrium point is unstable. The equilibrium point will be considered Lyapunov stable. If the condition  $\dot{E}(\mathbf{x})$  is not identically zero along any solution of  $\mathbf{x}$  for other than the equilibrium point then that equilibrium point is locally asymptotically stable. If also the entire state space of a positive-definite function  $E(\mathbf{x})$  that is radically unbounded,  $E(\mathbf{x}) \rightarrow \infty$  as  $|\mathbf{x}| \rightarrow \infty$  then the equilibrium point will be globally asymptotically stable for any initial condition [52].

### Equilibria of the System Describing Algal Growth

Solving the third order ODE in 2.11, 2.12, and 2.13 presents a solution that does not change with time. This equilibrium of the system, when put back into the system, will



produce a steady state result. The stability of these equilibrium points are evaluated by determining the eigenvalues of the Jacobian matrix  $A$  in 2.32. The real part of the eigenvalue needs to be negative and non repeating, giving the system asymptotic stability. This method is used to evaluate the stability of a nonlinear system.

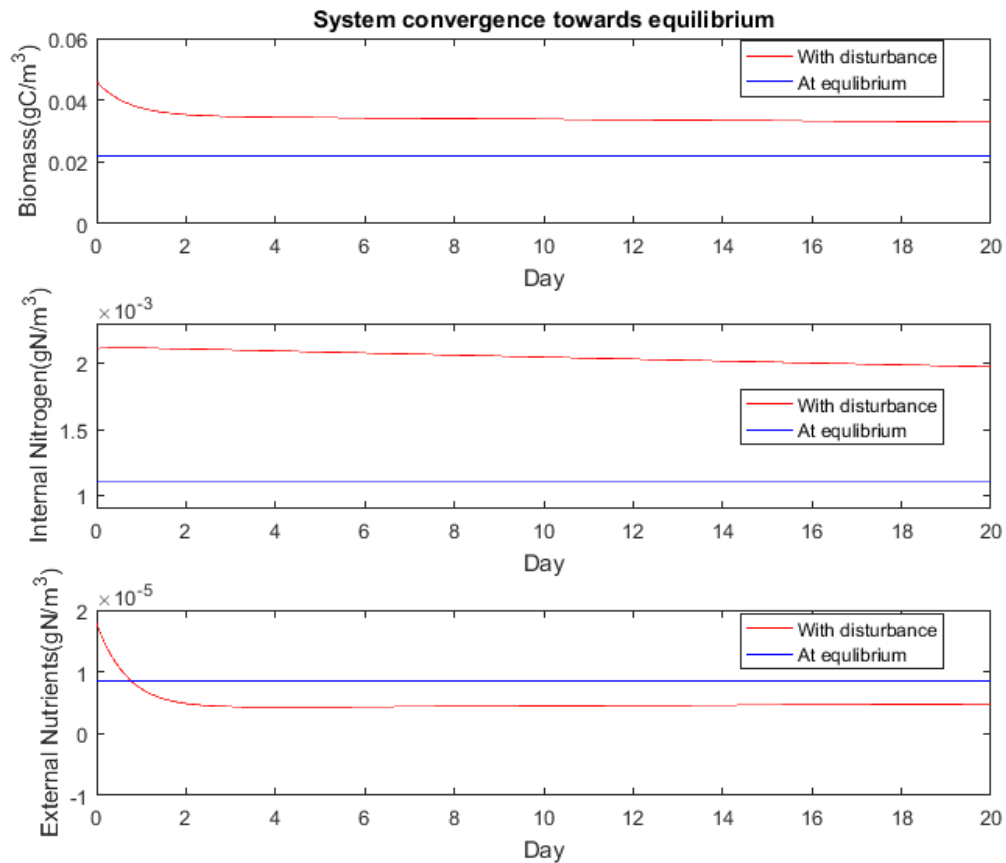


Figure 2.1: Equilibrium of System With a Small Disturbance

When the equilibrium points are used as initial conditions in the system, it will stay in that steady state. When this equilibrium is disturbed say at  $x(t = 0) = x^* + de$  instead of  $x(t = 0) = x^*$  the system will jump but then head towards convergence near the equilibrium, as demonstrated in Figure 2.1.

### 2.2.3 Linearization of the Algae Growth Model System

The system described by 2.19 is linearized and the Jacobian matrix  $A$  is built with the following equilibrium points.

$$x_1^* = \frac{N}{\bar{\lambda} \left( \frac{x_3^*}{x_3^* + K_3} \right) \left( 1 - \frac{\alpha}{Q_l} \right)} \quad (2.28)$$

$$x_2^* = \alpha x_1^* \quad (2.29)$$

$$x_3^* = \frac{R\alpha K_3}{\bar{\lambda} \left( 1 - \frac{\alpha}{Q_l} \right) - R\alpha} \quad (2.30)$$

where

$$\alpha = \frac{\gamma Q_o}{\gamma - R}. \quad (2.31)$$

The equilibrium points were applied to the Jacobian Matrix  $A$

$$A = \begin{bmatrix} \frac{\partial F_1}{\partial x_1} & \frac{\partial F_1}{\partial x_2} & \frac{\partial F_1}{\partial x_3} \\ \frac{\partial F_2}{\partial x_1} & \frac{\partial F_2}{\partial x_2} & \frac{\partial F_2}{\partial x_3} \\ \frac{\partial F_3}{\partial x_1} & \frac{\partial F_3}{\partial x_2} & \frac{\partial F_3}{\partial x_3} \end{bmatrix} \quad (2.32)$$

where the system specific Jacobian is

$$A = \begin{bmatrix} \gamma - \frac{2Q_o x_1}{x_2} - R & -\frac{2Q_o x_1 x_2 - Q_o x_1^2}{x_2^2} & 0 \\ \frac{\bar{\lambda} x_3}{x_3 + K_3} & -\frac{\bar{\lambda} x_3}{(x_3 + K_3) Q_l} - R & \frac{\bar{\lambda} x_1 K_3}{(x_3 + K_3)^2} - \frac{\bar{\lambda} Q_l x_2 K_3}{((x_3 + K_3) Q_l)^2} \\ -\frac{\bar{\lambda} x_3}{x_3 + K_3} & \frac{\bar{\lambda} x_3}{x_3 + K_3} & -\frac{\bar{\lambda} x_1 K_3}{(x_3 + K_3)^2} + \frac{\bar{\lambda} Q_l x_2 K_3}{((x_3 + K_3) Q_l)^2} \end{bmatrix} \quad (2.33)$$

so the eigenvalues for the system can be computed.

### 2.2.4 Sliding Mode Phenomenon in Dynamical Systems

Sliding mode phenomenon was first discovered in variable structure control systems, but recently other applications of sliding mode have been used. This section provides an explanation on sliding mode and will discuss how it will be used for designing observers and how this observer will be applied to an algal system. Sliding mode was first implemented as a high speed switched feedback, a form of discontinuous nonlinear control, and was applied to alter the dynamics of a nonlinear system by use of a high-frequency "switching control" [49]. Sliding mode will be explained using a first order system. Given a system

$$\dot{x} = -M \operatorname{sgn}(x) \quad M > 0 \quad (2.34)$$

where

$$\operatorname{sign}(x) = \begin{cases} -1 & x \leq 0 \\ +1 & x > 0 \end{cases} \quad (2.35)$$

if the initial condition  $x_o > 0$  then  $x(t) = -Mt + x_o$  so  $x(t)$  will decrease until  $x(t) = 0$ . If  $x_o < 0$  then  $x(t) = Mt + x_o$  and  $x(t)$  will increase until it reaches zero too as can be shown in Figure 2.2.

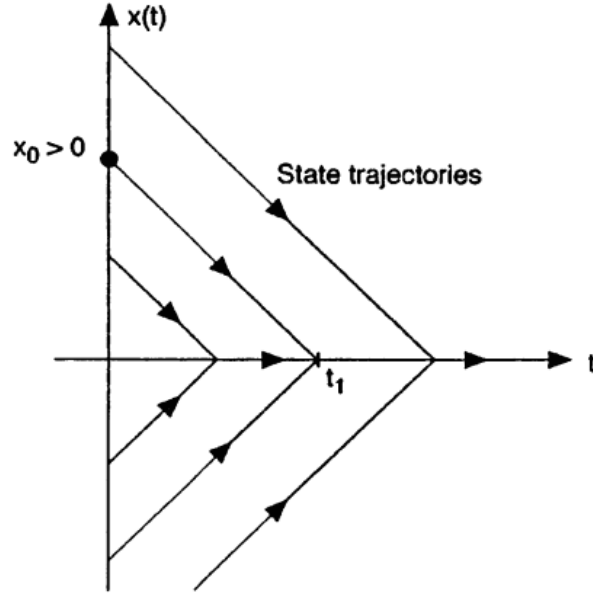


Figure 2.2: State trajectories for  $\dot{x} = -\text{sign}(x)$  [17]

This application of the discontinuous control signal forces the system to slide along a cross section of the system's normal behavior [25]. In practical implementation of a system (for example using discretization) the  $\text{sign}$  function will be switching from  $+1$  to  $-1$  with a sampling frequency and  $x(t) \approx 0$  for  $t \geq t_1$ . Now apply this to a nonlinear system  $f(x)$  such that

$$\dot{x} = -M \text{sgn}(x) + f(x) \quad |f| < M \quad (2.36)$$

the same will happen if  $|f| < M$  where  $x(t) = 0$  for  $t \geq t_1$ . Consider a nonlinear system with a control described by

$$\dot{x} = f(t, x) + B(t, x)u(x, t), \quad x \in R^n, u \in R^m \quad B \in R^{n \times m} \quad (2.37)$$

with a switching feedback control law

$$u_i = \begin{cases} u_i^+(t, x) & \sigma(x) > 0 \\ u_i^-(t, x) & \sigma(x) < 0 \end{cases} \quad i = 1, \dots, m \quad (2.38)$$

$u_i$  can be expressed as

$$u_i = \frac{u_i^+ + u_i^-}{2} + \frac{u_i^+ - u_i^-}{2} \text{sgn}(\sigma_i) \quad (2.39)$$

Meaning that after some time,  $x(t) \equiv 0$  when  $t \geq t_1$ . All trajectories from any initial conditions will converge to zero and there are no trajectories leaving zero. that means without loss of generality we can always assume

$$u_i = -M \text{sgn}(\sigma_i) \quad (2.40)$$

or

$$u = -M(t, x) \text{sgn}(\sigma) \quad \text{sgn}(\sigma) = [\text{sgn}(\sigma_1), \dots, \text{sgn}(\sigma_m)]^T \quad (2.41)$$

The problem is to find such switching function  $\sigma(x)$  so that  $\sigma(x(t)) \equiv 0$  for  $t \geq t_1$  is the sliding surface and it leads to  $x(t) \rightarrow 0$  where  $t \rightarrow \infty$  as illustrated in Figure 2.3.

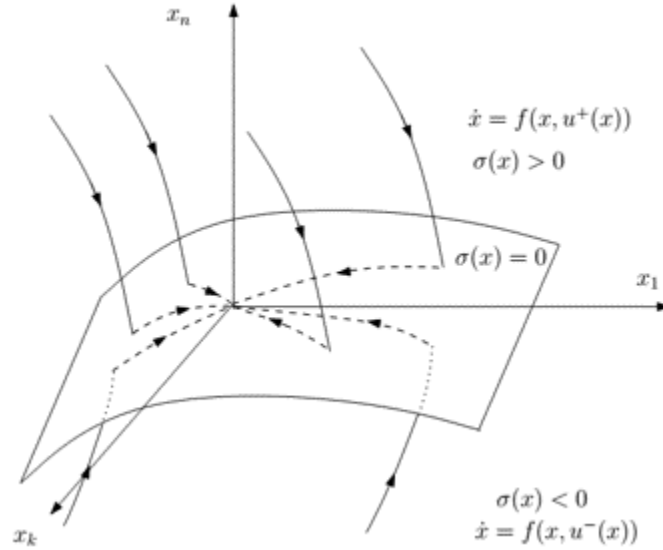


Figure 2.3: Sliding mode control for an on and off control system [33]

### Equivalent Control

When sliding mode starts at  $\sigma(x) \equiv 0$  the discontinuous control is switching with high frequency. The average value of this control is called equivalent control. Differentiating  $\sigma$  along the system trajectory using the chain rule we have

$$\dot{\sigma} = \frac{\partial \sigma}{\partial t} + \frac{\partial \sigma}{\partial x} \dot{x} = \frac{\partial \sigma}{\partial t} + \frac{\partial \sigma}{\partial x} f(x, t) + \frac{\partial \sigma}{\partial x} B(x, t) u_{eq} \quad (2.42)$$

If  $\sigma(x(t)) \equiv 0$  then  $\dot{\sigma} \equiv 0$  so

$$\frac{\partial \sigma}{\partial t} + \frac{\partial \sigma}{\partial x} f + \frac{\partial \sigma}{\partial x} B u = 0 \quad (2.43)$$

If  $\frac{\partial \sigma}{\partial x} B(x, t)$  is nonsingular for all of  $x$  and  $t$ , then  $u_{eq}$  can be computed as

$$u_{eq} = -\left[\frac{\partial \sigma}{\partial x} B(x, t)\right]^{-1} \left(\frac{\partial \sigma}{\partial t} + \frac{\partial \sigma}{\partial x} f(x, t)\right) \quad (2.44)$$

This equation can be used to extract new information about unmeasured disturbances or unmeasured states. On one hand  $u_{eq}$  can be obtained by finding the average of

discontinuous functions, on the other hand 2.42 allows us to express the unknown qualities using  $u_{eq}$ .

## 2.3 Linear System Observer Theory

In many control systems, designs are usually based off the state vector feedback where the system's inputs are functions only of the current state vector[37]. Given a linear system of the form

$$\dot{x} = Ax + Bu \quad x \in R^n \quad (2.45)$$

for example, 2.45 full state feedback allowing to stabilize  $x$  to zero is

$$u = -K\hat{x} \quad u \in R^r \quad (2.46)$$

But in many cases full state vector is no accessible but on some output

$$y = Cx \quad y \in R^m \quad (2.47)$$

is available. The problem is to calculate  $x(t)$  while measuring only  $y(t)$ . Whether  $y(t)$  has enough information about  $x(t)$  is a question of observability.

### 2.3.1 System Observability

Consider a linear time invariant system in state-space of the form,

$$\dot{x} = Ax + Bu \quad (2.48)$$

$$y = Cx \quad (2.49)$$

where  $x \in R^n$   $u \in R^r$  and  $y \in R^m$  and  $y$  describes the output vector for the measured states.

In order to determine the observability of the system, equations 2.48 and 2.49 can be tested with an observability matrix ( $rn \times n$ ) of the form

$$O = \begin{bmatrix} C \\ AC \\ A^2C \\ \vdots \\ A^{n-1}C \end{bmatrix} \quad (2.50)$$

The system is observable when  $O$  is full rank  $n$  [52]. In case for the system described in Equations 2.11, 2.12, and 2.13, where  $n = 3$  for the system, the rank of the observability matrix must also be 3 in order for the system to be observable.

### 2.3.2 Linear State Observers

The idea of the observer is to use system model with additional correction terms based on the measured output of the system. Looking at an asymptotic state observer in the form,

$$\dot{\hat{x}} = A\hat{x} + Bu + L(y - C\hat{x}) \quad (2.51)$$

where  $\hat{x}$  describes the estimate of  $x$ , and  $L$  denotes a gain matrix with dimensions  $n \times r$ , this is known as a Luenberger Observer. The corresponding error between the actual state and estimated state to be,

$$\bar{x} = x - \hat{x}. \quad (2.52)$$

The estimate error equation for  $\bar{x}$ , can then be described as,

$$\dot{\bar{x}} = (A - LC)\bar{x} \quad (2.53)$$

In order to drive the error,  $\bar{x}$  to zero, the eigenvalues of  $(A - LC)$  need to have negative real parts [52]. An example of a Luenberger observer is shown in Figure 2.4



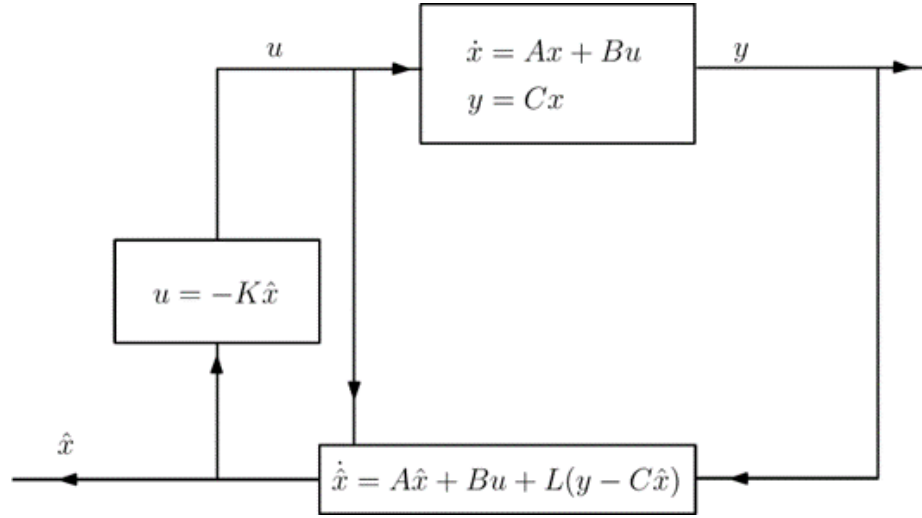


Figure 2.4: Block diagram of a Luenberger Observer[7] [33]

This observer does not take into account measurement noise and parameter uncertainties. It does however, demonstrate estimation error stability under optimal conditions [7].

### Proportional-Integral Observer

We know the Luenberger observer focuses on correcting the estimations with a term related to the difference between the actual outputs and predicted outputs as shown in 2.52. The Proportional Integral, or PI observer will use the integral of the error term[11] where the PI observer for the system in 2.51 will be re written as

$$\hat{\dot{x}} = Ax(t) + Bu(t) + K_I(y - C\hat{x}(t)) + K_P \int_0^t (y(\tau) - C\hat{x}(\tau)) \quad (2.54)$$

and where the error equation is now

$$e_x = x - \hat{x} \quad e_\omega = \int_0^t (y - C\hat{x})d\tau \quad (2.55)$$

so now

$$\begin{pmatrix} \dot{e}_x \\ \dot{e}_\omega \end{pmatrix} = \begin{pmatrix} A + K_I C & K_P \\ C & 0 \end{pmatrix} \begin{pmatrix} e_x(t) \\ e_\omega(t) \end{pmatrix} \quad (2.56)$$

where the gains  $K_I$  and  $K_P$  can be chosen to ensure stable error dynamics[6],[11]. This integrator will give the observer of the system more robustness in order to deal with the modeling uncertainties and the inherent measurement noise.

### 2.3.3 Kalman-Bucy Filter

Kalman filters are extremely popular for state estimation of linear systems since they are very similar to a Luenberger observer, but they utilize a time-varying gain. This will allow the variance in the error estimate to be minimized[11]. Given the observable system

$$\dot{\hat{x}}(t) = Ax(t) + Bu(t) + w(t); \quad x(t_o) = x_o \quad (2.57)$$

and

$$y(t) = Cx(t) + v(t) \quad (2.58)$$

where the centered white noises, or Gaussian perturbations, of the system are represented by  $w(t)$  and  $v(t)$  [4] and assuming the initial distribution is also Gaussian with initialization described as

$$E(x_o) = \tilde{x}_o; \quad E((x_o - \tilde{x}_o)(x_o - \tilde{x}_o)^T) = P_o \quad (2.59)$$

the Kalman-Bucy filter gives the state estimation vector to be optimal in a quadratic sense of  $E\|x - \hat{x}\|^2 \rightarrow E(\hat{x})$

$$\dot{\hat{x}}(t) = A\hat{x}(t) + Bu(t) + K(t)[y(t) - C\hat{x}(t)]; \quad \hat{x}(t_o) = \hat{x}_o \quad (2.60)$$

with the covariance error propagation

$$P(t) = E[(x - \hat{x})(\hat{x} - \hat{x})^T] \quad (2.61)$$

so

$$\dot{P}(t) = AP(t) + P(t)A^T - P(t)C^T R(t)^{-1}CP(t) + Q(t) \quad (2.62)$$

where  $Q(t)$  and  $R(t)$  are Gaussian covariances with respect to  $w(t)$  and  $v(t)$  [11]. the gain,  $K(t)$ , can be computed to be

$$K(t) = P(t)C^T R(t)^{-1} \quad (2.63)$$

This filter can be applied when matrices  $A$  and  $C$  are time dependent[11] Sliding mode can be used for state estimation and can be applied to linear and nonlinear systems.

### 2.3.4 Sliding Mode Observer for Linear System

Sliding Mode observer uses a discontinuous function of the difference between outputs of the system and the observer. In the linear case, instead of a linear correcting term like the Luenberger observer, it uses a discontinuous feedback function based on the output of the linear function with a discontinuous function[18] shown as

$$\dot{\hat{x}} = A\hat{x} + Bu + Lsign(y - C\hat{x}) \quad (2.64)$$

where  $y$  is described in equation 2.49; using the gain matrix  $L$  sliding will occur in the system 2.64 on the manifold  $y - C\hat{x} = 0$ , and it will become equivalent to the reduced order observer[18], where  $sign$  is a high speed feedback discontinuous function that will drive the state of a system to a predetermined sliding surface in state-space shown as[22],

The linear sliding mode observer was introduced by [21] and has been well developed for the case of linear systems. The observer has a structure composed of the system model with additional inputs that are used to steer the output of the observer to the measured output of the estimated system.

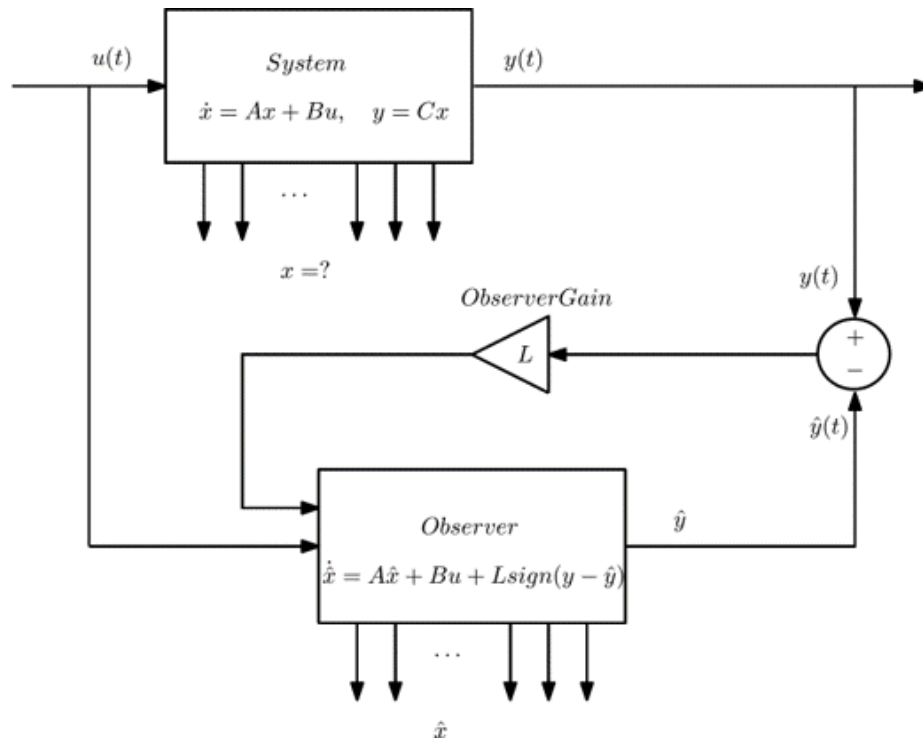


Figure 2.5: Block Diagram of a Linear Sliding Mode Observer  
[33]

Shown in Figure 2.5 with the observability condition, the system and the state of the observer are approximately equal to the state of the real-life system, thereby providing estimates of the variables that are not measured directly[20].

There are many approaches to applying observers to nonlinear systems, this sliding mode approach is one that can be applied to a variety of systems.

## 2.4 Nonlinear Observer Theory

Originally nonlinear observers were developed based on the idea of variable structure control for the use of detecting disturbances in complex systems[24]. In practice, having all state variables available for direct measurement is extremely rare. For the case of linear systems, observers have been developed extensively in the form of Luenberger observers as well as PI observers and Kalman-Buchy filters. In the field of

nonlinear systems, a nonlinear observer design is considerably more challenging and has been the center of attention in a lot of research practices.

For nonlinear continuous-time systems, observers such as the extended Luenberger observer and the Extended Kalman Filter have been used. These approaches are very robust when disturbances are implemented and measurement noise is monitored. For the case of continuous-time state estimation from discrete-time measurement, a two stage implementation can be used. The predictor state reconstructs the state vector by validating the numerical integration methods to drive the guaranteed numerical evaluation of the solution to the ODEs at determined measurement time steps[29]. The correction stage consisting of the feasible domain of the measured output and the simulated output are compared in order to minimize the estimated state vector from the prediction stage. The second stage looks at a continuous-time state estimation for continuous-time measurements, where a closed loop interval observer takes the model's parameters' uncertainties into account. A lower and upper bound are computed for the state vector, which limits all possible state vectors generated by the uncertainty in the system and are consistent with the measured data[29].

### 2.4.1 Extended Kalman Filter

The most popular state estimator for nonlinear systems is the extended Kalman filter, which is based on the model linearization along the estimated trajectory that will make it suboptimal [39], [28]. In the case of a continuous-discrete system with additive noise shown as

$$\dot{x}(t) = f(x(t), u(t)) + \eta(t) \quad y(t_k) = h(x(t_k)) + \epsilon(t_k) \quad (2.65)$$

where  $(x_t) = x_0$ ,  $\eta(t)$  and  $\epsilon(t_k)$  are normally distributed white noises. The corresponding estimation of the state vector is [11]

$$\dot{\hat{x}}(t) = \hat{f}(\hat{x}(t)) + K(t)[y(t) - h(\hat{x}(t))] \quad \hat{x}(t_o) = \hat{x}_o \quad (2.66)$$

The extended Kalman filter will provide an estimation of the mean and covariance matrix of the state vector and its equations[28]. This example does not take into

account parameter and input uncertainties.

### 2.4.2 Nonlinear Sliding Mode Observer

Now consider a nonlinear system of the form,

$$\dot{x} = f(x, t) \quad (2.67)$$

where  $y$  is the output vector measurements

$$y = h(x) \quad (2.68)$$

where  $x \in R^n$ .  $y \in R^m$  where  $m = 1$  with

$$f(x) = \begin{bmatrix} f_1(x) \\ f_2(x) \\ f_3(x) \\ \vdots \\ f_n(x) \end{bmatrix} \quad (2.69)$$

The sliding mode observer can be designed in terms of the estimated states of the system. In order to estimate the state in system 2.67 by measurements in 2.68 the observer takes the following form[19].

$$\hat{\dot{x}} = \left[ \frac{\partial H(x)}{\partial x}(\hat{x}) \right]^{-1} M(\hat{x}) \operatorname{sgn}(V(t) - H(x)) \quad (2.70)$$

Where  $H(x)$  is a column vector that is built as an output function for  $h(x)$  and its corresponding Lie derivatives

$$H(x) = \begin{bmatrix} h_1(x) \\ h_2(x) \\ h_3(x) \\ \vdots \\ h_n(x) \end{bmatrix} = \begin{bmatrix} h(x) \\ L_f h(x) \\ L_f^2 h(x) \\ \vdots \\ L_f^{n-1} h(x) \end{bmatrix} = \begin{bmatrix} h(x) \\ \frac{\partial h_1(x)}{\partial x} f(x) \\ \frac{\partial h_2(x)}{\partial x} f(x) \\ \vdots \\ \frac{\partial h_{n-1}(x)}{\partial x} f(x) \end{bmatrix} \quad (2.71)$$

where  $L_f^i$  is the  $i$ th Lie derivatives applied to equation 2.68 which is the output function along system  $f$  [19]. The following  $M(\hat{x})$  matrix is a diagonal  $n \times n$  matrix of gains shown with positive elements  $m_i(x), i = 1, \dots, n$ [18].

$$M(\hat{x}) = \begin{bmatrix} M_1(\hat{x}) & & & & \\ & M_2(\hat{x}) & & & \\ & & M_3(\hat{x}) & & \\ & & & \ddots & \\ & & & & M_n(\hat{x}) \end{bmatrix} \quad (2.72)$$

$M_i(\hat{x}) > 0$  must be large enough to progress towards sliding mode [35].

$V(t)$  is shown to be

$$V(t) = \begin{bmatrix} v_1(t) \\ v_2(t) \\ v_3(t) \\ \vdots \\ v_n(t) \end{bmatrix} = \begin{bmatrix} y(t) \\ [L_1(\hat{x})\text{sign}(v_1(t) - h_1(\hat{x}))]_{eq} \\ [L_2(\hat{x})\text{sign}(v_2(t) - h_2(\hat{x}))]_{eq} \\ \vdots \\ [L_n(\hat{x})\text{sign}(v_{n-1}(t) - h_{n-1}(\hat{x}))]_{eq} \end{bmatrix} \quad (2.73)$$

This method possess two drawbacks. First, the observer vector  $V(t)$  is determined by each successive step of taking the equivalent value, which potentially leads to chattering noise produced by a finite frequency of the feature switching in the sliding mode observer [35]. The other features is the Jacobian matrix,  $H(\hat{x})$  and  $\frac{\partial H(\hat{x})}{\partial x}$ , must stay nonsingular in order to be invertible[35]. The non-singularity of the Jacobian is actually the observability condition.

The observer convergence can be proved by considering the modified error

$$e(t) = H(x) - H(\hat{x}) \quad (2.74)$$

using 2.67 and 2.68 we obtain

$$\dot{e} = \frac{\partial H}{\partial x}(x)\dot{x} - \frac{\partial H}{\partial x}(\hat{x})\dot{\hat{x}} = \frac{\partial H}{\partial x}(x)f(x) - \frac{\partial H}{\partial x}(\hat{x}) \left[ \frac{\partial H}{\partial x}(\hat{x}) \right]^{-1} \quad (2.75)$$

which is

$$\dot{e} = \frac{\partial H}{\partial x}(x)f(x) - M(x)\text{sgn}(V(t) - H(\hat{x})) \quad (2.76)$$

$$\begin{bmatrix} \dot{e}_1 \\ \dot{e}_2 \\ \vdots \\ \dot{e}_i \\ \vdots \\ \dot{e}_{n-1} \\ \dot{e}_n \end{bmatrix} = \begin{bmatrix} \dot{h}_1(x) \\ \dot{h}_2(x) \\ \vdots \\ \dot{h}_i(x) \\ \vdots \\ \dot{h}_{n-1}(x) \\ \dot{h}_n(x) \end{bmatrix} - M(\hat{x})\text{sgn}(V(t) - H(\hat{x}(t))) = \begin{bmatrix} h_2(x) \\ h_3(x) \\ \vdots \\ h_{i+1}(x) \\ \vdots \\ h_n(x) \\ L_f^n h(x) \end{bmatrix} - \begin{bmatrix} m_1 \text{sgn}(v_1(t) - h_1(\hat{x}(t))) \\ m_2 \text{sgn}(v_2(t) - h_2(\hat{x}(t))) \\ \vdots \\ m_i \text{sgn}(v_i(t) - h_i(\hat{x}(t))) \\ \vdots \\ m_{n-1} \text{sgn}(v_{n-1}(t) - h_{n-1}(\hat{x}(t))) \\ m_n \text{sgn}(v_n(t) - h_n(\hat{x}(t))) \end{bmatrix} \quad (2.77)$$

As long as  $m_1(\hat{x}) \geq |h_2(x(t))|$  the first row in the error dynamics  $\dot{e}_1 = h_2 - m_1(\hat{x})\text{sgn}(e_1)$  will be sufficient enough as a condition to enter  $e_1 = 0$  for a sliding mode in finite time. Along the  $e_1 = 0$  surface, the corresponding  $v_2(t) = [m_1(\hat{x})\text{sgn}(e_1)]_{eq}$  equivalent control will be equal to  $h_2(x)$  and so  $v_2(t) - h_2(\hat{x}) = h_2(x) - h_2(\hat{x}) = e_2$ , where the second row in the error dynamics  $\dot{e}_2 = h_3(\hat{x}) - m_2(\hat{x})\text{sgn}(e_2)$  will enter the  $e_2 = 0$  sliding mode in finite time [19]. Where along the  $e_i = 0$  surface, the corresponding  $v_{i+1} = [\dots]_{eq}$  equivalent control will be equal to  $h_{i+1}(x)$ , so as long as  $m_{i+1} \geq |h_{i+2}(x(t))|$  the  $(i+1)^{th}$  row in the error dynamics will enter  $e_{i+1} = 0$  sliding mode in finite time [19]. When the gains  $m_i$  are large, all observer estimated states reach the actual states in the finite time. Meaning, increasing  $m_i$  will allow for faster convergence in any desired finite time as long as each  $h_i(x(0))$  function can be bounded [19], emphasizing the Jacobian of  $H(x)$  must be invertible.

### 2.4.3 Problem Setup

The goal of this thesis is to apply a nonlinear sliding mode observer to estimate parameters such as algae biomass, internal nitrogen, and external nutrients described by Droop's model for microalgae growth derived from a 2D coupled hydrodynamic and biological model described in [10].



### Simulation Parameters

Parameters used to model algae growth can be found in Table A.1 located in Appendix A. The controlled external nitrate values used for the model first had initial conditions set to  $9\mu gN/m^3$ , but unfortunately this does not produce algae concentrations that resemble the model in [10] When the initial conditions into the model are changed, for example, using  $20gC/m^3$  for biomass and  $5gN/m^3$  for internal nitrogen and external nitrates the system will respond in a more realistic manner that closely follow [10].

### Model Validation

The algae growth model is compared with concentration values described in [10]. After removing the spatially dependent terms and assuming the algae is sitting on the surface of the water, the growth curve presented in the results still falls on the same order of magnitude as [10].

When analyzing the observability and stability of the equilibrium of the  $3^{rd}$  order non-linear system, the rank of the concatenated matrix  $O$  needs to match the rank of the system in order for the system to be observable and the equilibrium need to be locally asymptotically stable. The stability of the nonlinear system was analyzed through the method of linearization and when the eigenvalues of the Jacobian matrix of the linearized system have all negative and non-repeating real parts the linearized system is globally asymptotically stable and the nonlinear system is locally asymptotically stable.

# Chapter 3

## Results

### 3.1 Simplified Droop Model Results

The simulation results for the simplified Droop Model derived from [10] are presented. The system illustrated by Equations 2.15, 2.16, and 2.17 are solved using Euler's method with a sufficiently small time step  $dt$  was needed to provide fast parameter modeling in the system over the span of ten days. The simulation results for the simplified model are presented below.

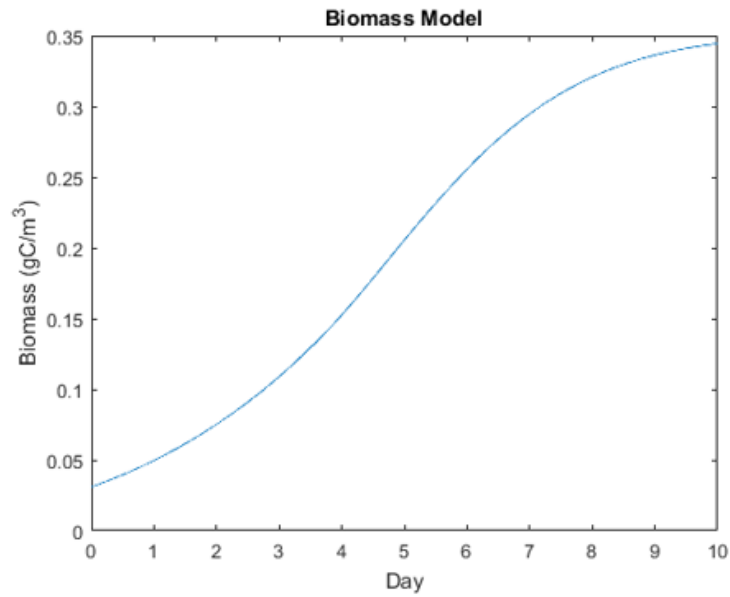


Figure 3.1: Algae growth demonstrated by Droop's Model

The algae growth in Figure 3.1 represents growth simulated in a petri dish under a growth lamp. The initial conditions for this growth are the equilibrium of the system with some small disturbance  $de = 0.001$ . The corresponding internal nitrogen and external nutrients are presented in Figures 3.2 and 3.3

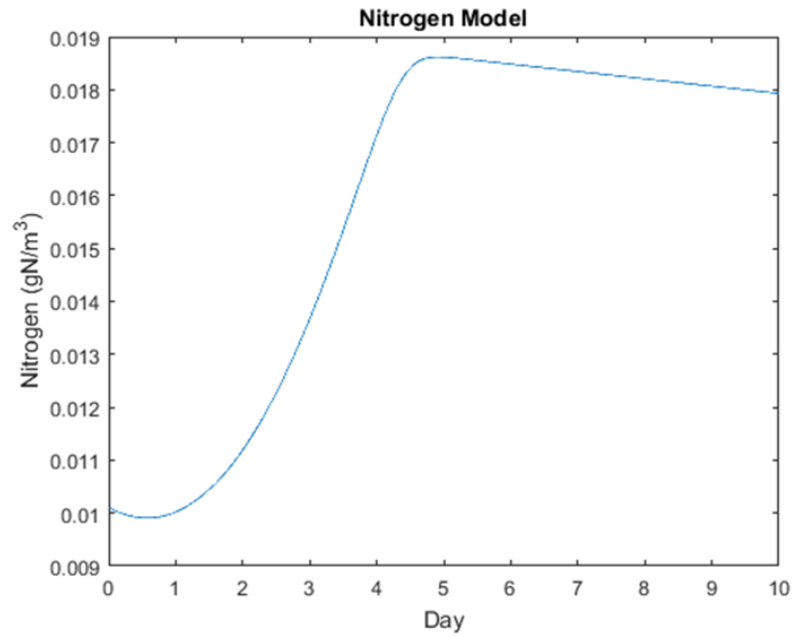


Figure 3.2: Internal nitrogen growth closely follows algae biomass growth

Figures 3.1 and 3.2 show the relationship between the algae biomass and the internal nitrogen. As the biomass grows the internal nitrogen will follow. Figure 3.3 shows the decrease in the available nutrients as the algae consumes them.

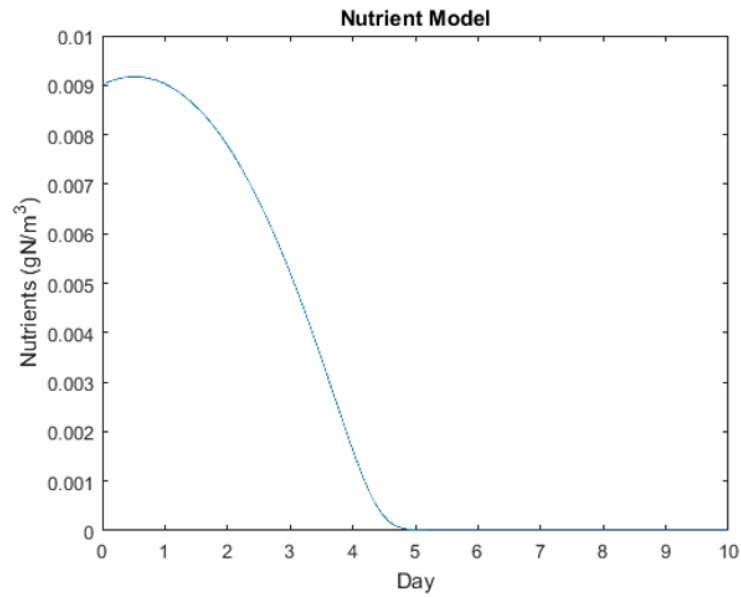


Figure 3.3: External nitrates ( $NO_3^-$ ) decrease when consumed by microalgae

Figures 3.1, 3.2, and 3.3 have initial conditions that are a small deviation, *de*, from the equilibrium point. The equilibrium points are extremely small, on the order of magnitude of milligrams of carbon for biomass and milligrams of nitrogen for internal nitrogen and external nitrates.

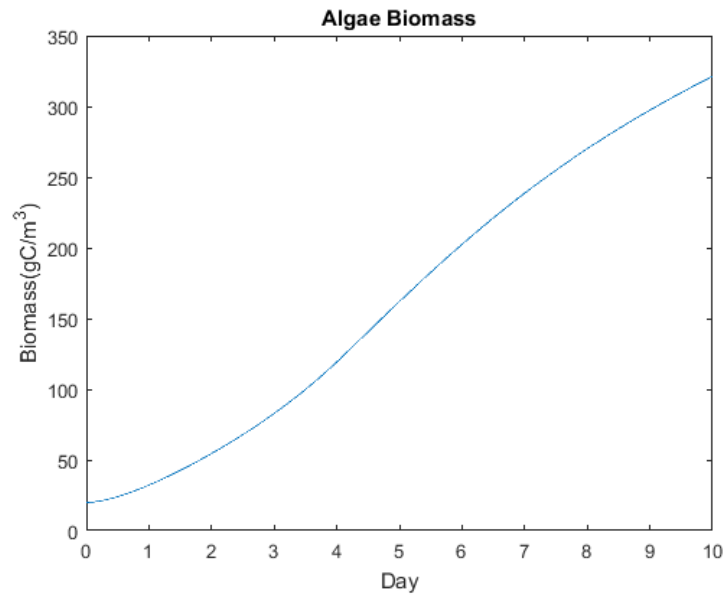


Figure 3.4: Algae biomass concentrations are more representative to nature

Figure 3.4 shows a more realistic representation of aglal concentrations and more closely follows [10]. This helps demonstrate the validity of the model where the growth of the algae is more representative of a natural growth given a flow of nutrients.

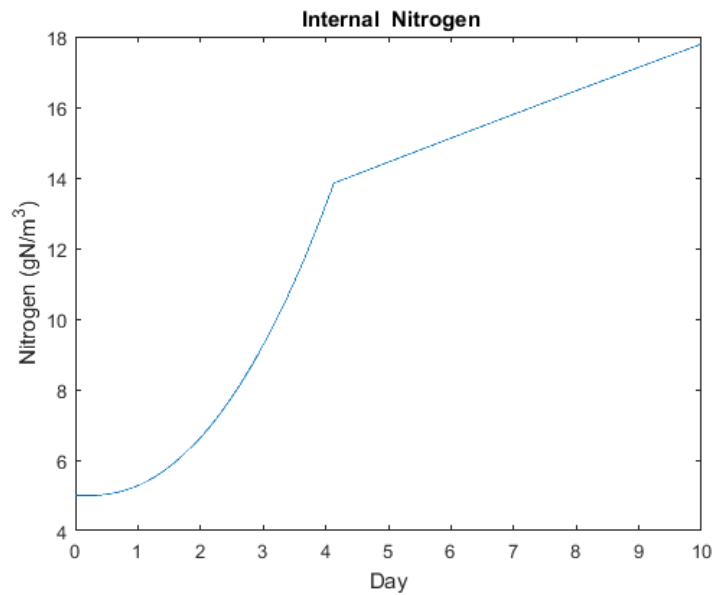


Figure 3.5: Internal Nitrogen

The amount of internal nitrogen in the biomass grew as well with higher initial conditions such as  $5 \frac{gN}{m^3}$ .

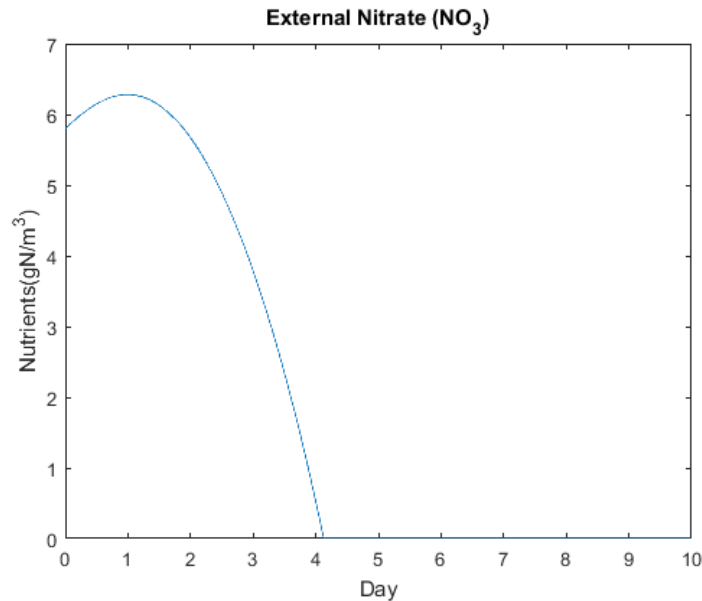


Figure 3.6: External Nitrate

When the new initial conditions are applied, the system demonstrates a more representative growth that follows [10]. When EPA water quality limits for allowable external nitrates in a water system are used for  $N$ , the system shows a realistic growth and response where the nitrates will be consumed after about four days and the algae will continue to grow as it consumes its internal nitrogen.

## 3.2 State Observers Applied to Microalgae System

This section will focus on the results from applications of linear observers and the algal system's response to disturbances from the equilibria.

### 3.2.1 Linear State Observer

State observers applied to the system in 2.15, 2.16, and 2.17 are presented. Algae biomass, internal nitrogen and external nitrates were observed. In the following figures, the black line represents the linear observer estimate of the observed parameter using a Luenberger Observer. The observer gains in  $L$  were found using the "acker" function in MATLAB which uses Ackermann's formula [32] to calculate the gains. The magenta line shows the linear sliding mode observer and red shows the system in its steady state.

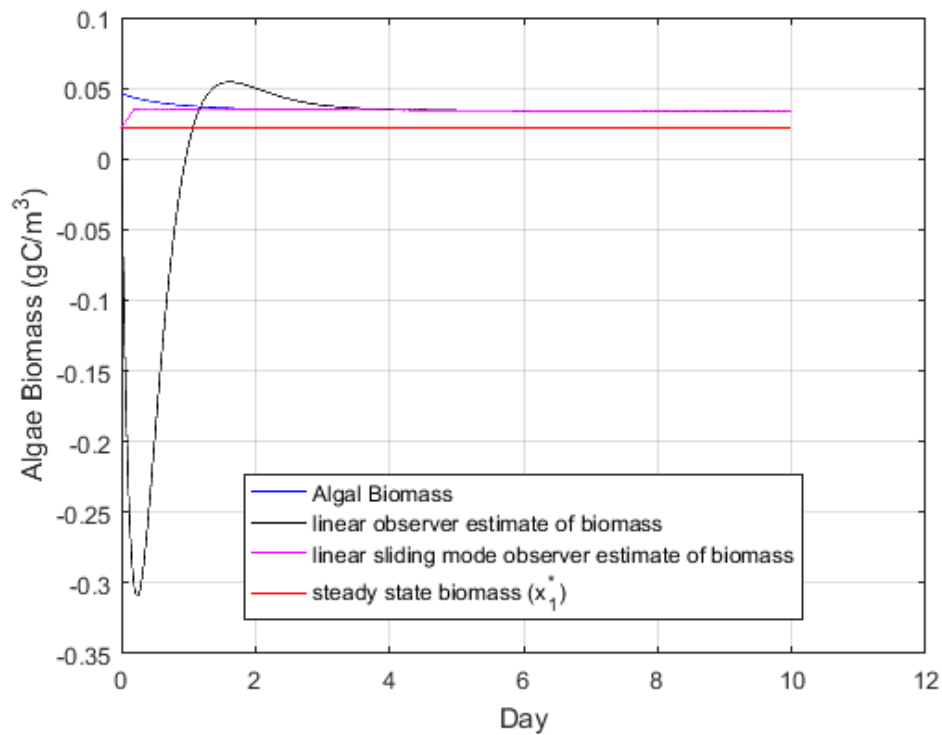


Figure 3.7: Linear State Observer for Biomass

The linear observer estimate for biomass in 3.7 takes the longest to converge towards the equilibria region while the linear sliding mode observer takes less time to converge.



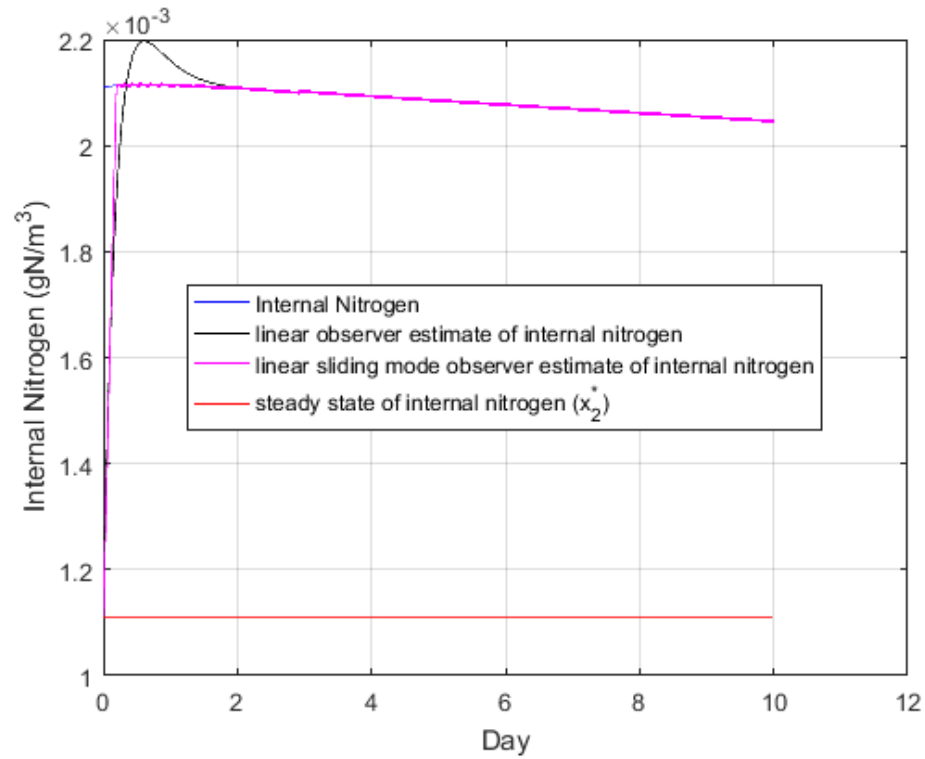


Figure 3.8: Linear State Observer for Internal Nitrogen

Figure 3.8 does not show successful convergence within ten days. However, if the time period is increased to about one thousand days, the system will converge and is shown in Figure 3.9.

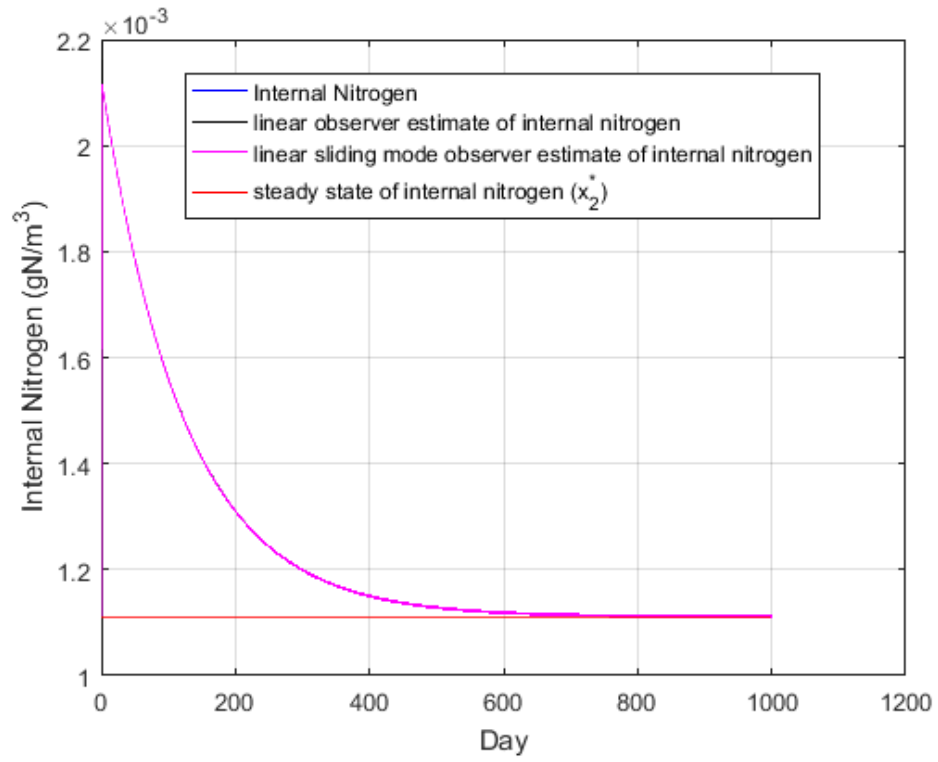


Figure 3.9: Linear State Observer for Internal Nitrogen Showing Convergence

Estimation of external nutrients show the linear sliding mode observer converges faster than the Luenberger observer.

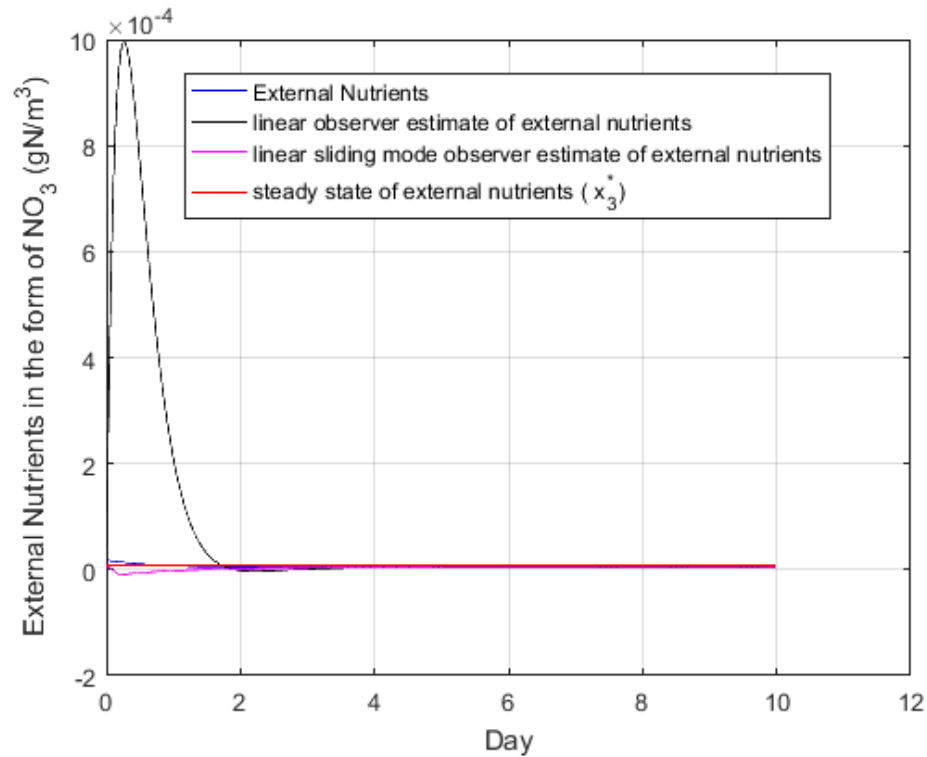


Figure 3.10: Linear State Observer for External Nutrients

Overall, the linear observers applied to a biological system that model algae biomass, internal nitrogen concentration, and nutrient concentration shows that the system converges fast for biomass and external nutrients but takes an extremely long time for internal nitrogen to converge. Since the goal of an observer is to have fast convergence towards the model, i.e. in a few days compared to the thousand days, this is not ideal for a linear observer. This demonstrates the need for the use of a nonlinear observer that is more robust to have a fast convergence towards the model. Figures 3.7, 3.8, and 3.10 illustrate the use of a linear Luenberger observer and a linear sliding mode observer applied to the linearized model demonstrating the success of applying linear state observers to a linearized system.

### 3.2.2 Nonlinear Sliding Mode Observer

Applying the nonlinear sliding mode observer to the system described in 2.15, 2.16, 2.17 where this system is of the form

$$\dot{x} = f(x) \quad (3.1)$$

Where  $f(x)$  can be noted as

$$f(x) = \begin{bmatrix} F_1(x) \\ F_2(x) \\ F_3(x) \end{bmatrix} = \begin{bmatrix} \dot{x}_1 \\ \dot{x}_2 \\ \dot{x}_3 \end{bmatrix} = \begin{bmatrix} \gamma \left(1 - \frac{Q_o x_1}{x_2}\right) x_1 - R x_1 \\ \bar{\lambda} \left(\frac{x_3}{x_3 + K_3}\right) \left(1 - \frac{x_2}{Q_l x_1}\right) x_1 - R x_2 \\ -\bar{\lambda} \left(\frac{x_3}{x_3 + K_3}\right) \left(1 - \frac{x_2}{Q_l x_1}\right) x_1 + N \end{bmatrix} \quad (3.2)$$

Constructing the  $H(x)$  vector

$$H(x) = \begin{bmatrix} h_1(x) \\ h_2(x) \\ h_3(x) \\ \vdots \\ h_n(x) \end{bmatrix} = \begin{bmatrix} h(x) \\ L_f h(x) \\ L_f^2 h(x) \\ \vdots \\ L_f^{n-1} h(x) \end{bmatrix} = \begin{bmatrix} h(x) \\ \frac{\partial h_1(x)}{\partial x} f(x) \\ \frac{\partial h_2(x)}{\partial x} f(x) \\ \vdots \\ \frac{\partial h_{n-1}(x)}{\partial x} f(x) \end{bmatrix} \quad (3.3)$$

where the components of  $H(x)$  are computed below

$$h_1(x) = x_2 \quad (3.4)$$

$$h_2(x) = \frac{\partial h_1(x)}{\partial x} f(x) = F_2 \quad (3.5)$$

$$h_3(x) = \frac{\partial h_2(x)}{\partial x} f(x) = \frac{\partial x_2}{\partial x_1} F_1 + \frac{\partial x_2}{\partial x_2} F_2 + \frac{\partial x_2}{\partial x_3} F_3 \quad (3.6)$$

The computation for the Jacobian of  $H(x)$  is shown below where  $\frac{\partial H(x)}{\partial x}$  is of the form

$$\frac{\partial H(x)}{\partial x} = \begin{bmatrix} 0 & 1 & 0 \\ \frac{\partial F_2}{\partial x_1} & \frac{\partial F_2}{\partial x_2} & \frac{\partial F_2}{\partial x_3} \\ \frac{\partial}{\partial x_1} h_3(x) & \frac{\partial}{\partial x_2} h_3(x) & \frac{\partial}{\partial x_3} h_3(x) \end{bmatrix} \quad (3.7)$$

where

$$\begin{aligned} \frac{\partial}{\partial x_1} h_3(x) = \frac{\bar{\lambda} x_3}{x_3 + K_3} \left[ \gamma - \frac{2\gamma x_1}{x_2} - 2R \right] + \frac{\bar{\lambda}}{(x_3 + K_3)^2} \left[ \frac{-\bar{\lambda} x_3^2}{Q_l} - 2\bar{\lambda} K_3 x_1 x_3 \right. \\ \left. + NK_3 \right] + \frac{2\bar{\lambda} K_3 x_3}{Q_l (x_3 + K_3)^3} \end{aligned} \quad (3.8)$$

$$\begin{aligned} \frac{\partial}{\partial x_2} h_3(x) = 2Rx_2 + \frac{\bar{\lambda} x_3}{x_3 + K_3} \left[ \frac{\gamma Q_o x_1^2}{x_2^2} + \frac{R}{Q_l} \right] + \frac{\bar{\lambda}}{Q_l (x_3 + K_3)^2} \left[ \frac{\bar{\lambda} x_3^2}{Q_l} - NK_3 \right] \\ + \frac{2\bar{\lambda} K_3 x_3}{Q_l (x_3 + K_3)^2} \left[ x_1 - \frac{x_2}{Q_l} \right] \end{aligned} \quad (3.9)$$

$$\begin{aligned} \frac{\partial}{\partial x_3} h_3(x) = \frac{\bar{\lambda} K_3}{(x_3 + K_3)^2} [-2\gamma x_1 - \gamma Q_o K_3 x_1^2 - 2Rx_1 + Rx_2] \\ + \frac{\bar{\lambda} K_3}{Q_l (x_3 + K_3)^2} [-2x_1^2 x_3 + Rx_2 + 2Nx_2] + \frac{2\bar{\lambda}^2 K_3 x_2 x_3}{Q_l^2 (x_3 + K_3)^2} \\ + \frac{\bar{\lambda} K_3 (x_3 - K_3)}{(x_3 + K_3)^3} [x_1^2 - N] + \frac{2\bar{\lambda}^2 K_3 x_1 x_2 (K_3 - 2x_3)}{Q_l (x_3 + K_3)^4} \\ - \frac{\bar{\lambda}^2 K_3 x_2^2 (K_3 - 2x_3)}{Q_l^2 (x_3 + K_3)^4} \end{aligned} \quad (3.10)$$

Since the inverse of 3.7 cannot be easily determined, an estimation of the inverse of 3.7 can be calculated using a transformation. Since the system is of the form

$$\dot{\hat{x}} = f(x) \quad (3.11)$$

where

$$y = h(x) = x_2 \quad (3.12)$$

the system can be transformed into an estimated state space where

$$\begin{aligned} y &= y_1 \\ \dot{y} &= y_2 \\ \ddot{y} &= y_3 \end{aligned} \quad (3.13)$$

so

$$\begin{aligned} \dot{y}_1 &= y_2 \\ \dot{y}_2 &= y_3 \\ \dot{y}_3 &= g(y_1, y_2, y_3) \end{aligned} \quad (3.14)$$

where  $H(x)$  will still be

$$H(x) = \begin{bmatrix} h(x) \\ L_f h(x) \\ L_f^2 h(x) \end{bmatrix} = \begin{bmatrix} y_1 \\ y_2 \\ y_3 \end{bmatrix} \quad (3.15)$$

where the sliding mode observer is still of the form

$$\dot{\hat{x}} = L \operatorname{sgn}(\hat{Y} - H(\hat{x})) \quad (3.16)$$

such that  $\hat{Y}$  is

$$\begin{aligned} \dot{\hat{y}}_1 &= L_1 \operatorname{sgn}(y - \hat{y}_1) = v_2 \\ \dot{\hat{y}}_2 &= L_2 \operatorname{sgn}(y - \hat{y}_2) = v_3 \\ \dot{\hat{y}}_3 &= L_3 \operatorname{sgn}(y - \hat{y}_3) = v_4 \end{aligned} \quad (3.17)$$

where the goal is to estimate  $y$  then find  $x$  by finding  $L$  such that  $\hat{Y} \rightarrow H(\hat{x})$ . This gives the result shown in Figure 3.11.

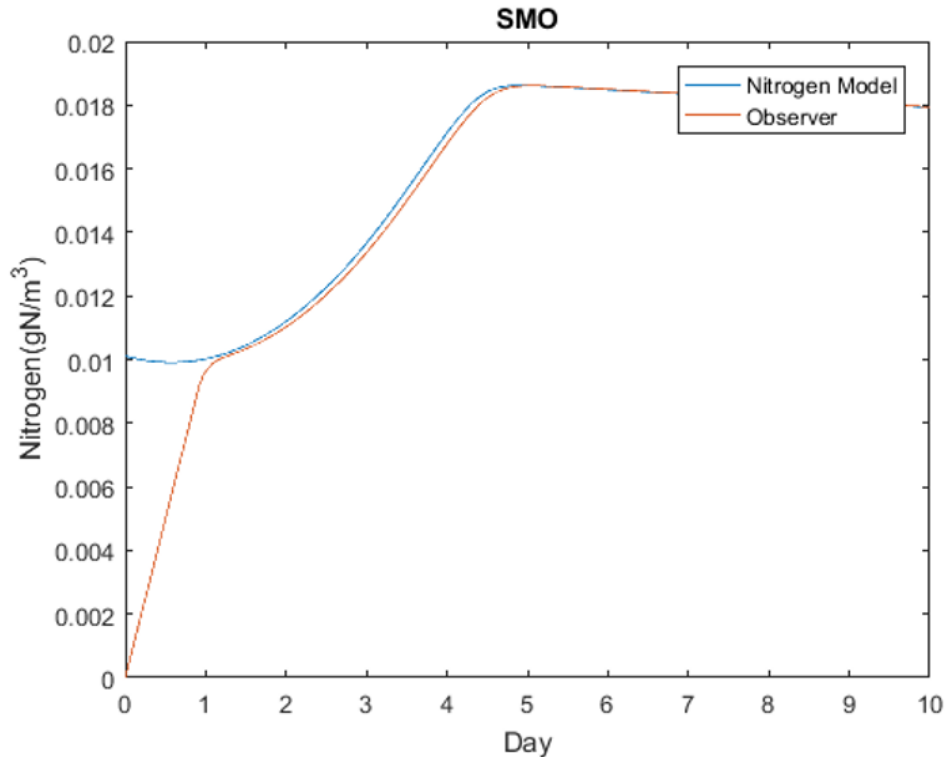


Figure 3.11: Sliding Mode Observer applied to internal nitrogen

The nonlinear sliding mode observer developed for this thesis successfully observed parameters of a simplified Droop Model describing algal growth. The trajectory of the observer makes sense, because the observer starts at zero, while the internal nitrogen has initial conditions, the observer will then successfully converge to the internal nitrogen and follow it. This takes less than a day compared to the linear observers used for internal nitrogen, which took approximately a thousand days.

### 3.3 Other Analysis

Monte Carlo simulations can be used to generate random disturbances to look at a system's response. Usually these random objects are introduced through computer

simulations in order to solve deterministic problems, which involves random sampling from certain probably distributions and can be applied to natural systems to see how a natural system responds to various disturbances[36]. A Monte Carlo simulation was applied to the biomass model with a uniformly distributed randomized disturbance from the equilibrium to observe the model's response.

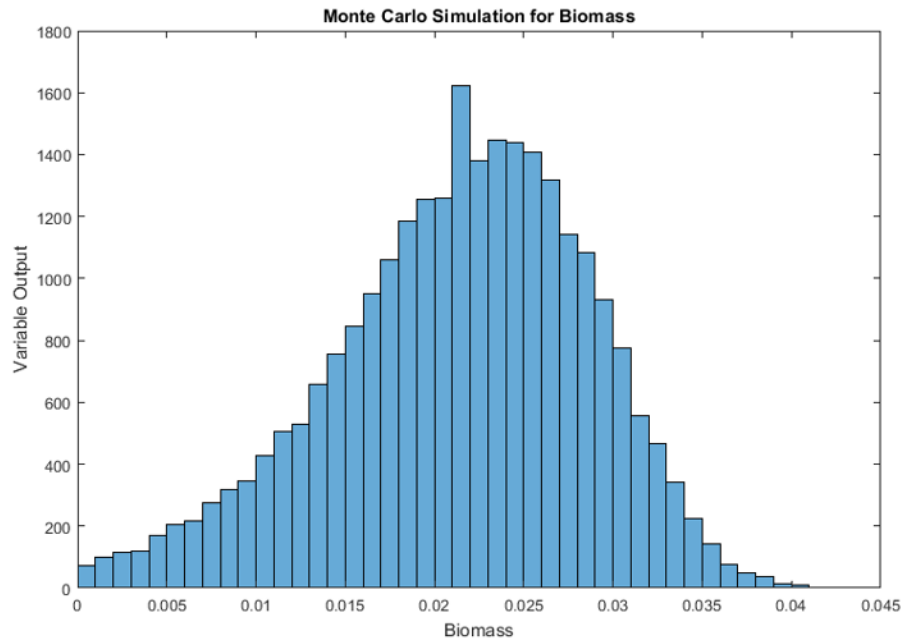


Figure 3.12: Monte Carlo simulation showing a distribution of biological model based off random inputs into the system.

The simulation results in Figure 3.12 show the system's response to randomized disturbances to the initial conditions. This was simulated over the system that illustrated the low algae concentration, meaning, the concentrations for algal biomass would not be measurable in an open system. This shows the system's behavior around the region near the equilibrium is normal.



# Chapter 4

## Conclusion and Discussion

### Simulation of Algae Growth

Figures 3.1, 3.2, and 3.3 describe algal growth with initial conditions that are near the equilibrium region. These values are very low, with initial concentration for algae biomass starting at approximately  $0.04 \frac{gC}{m^3}$  and only growing up till  $0.35 \frac{gC}{m^3}$ . These concentration values do not fall on the same order of magnitude for algae concentrations in [10] nor are they representative of the growth that occurs naturally. Figures 3.4, 3.5, and 3.6 demonstrate algae growth the more closely follows [10], where the concentration values are on the same order of magnitude. This represents algae growth more naturally, especially since the initial conditions start at higher concentration values.

### Discussion on System Sensitivity to Parameter and Initial Condition Changes

PDEs describing naturally occurring systems are extremely complicated. In order to develop models describing these systems, usually they are simplified in to an  $n$ th order ODE that are typically extremely nonlinear with each parameter coupled with the others. This simplification makes the system extremely sensitive to small parameter changes as well as changes to initial conditions. This occurred with the above simplified algal system. Initially the starting conditions were the equilibria of the system. When some small deviation was introduced the system would respond within

one or two orders of magnitude. When a small control input  $N$  was used, the system responded normally, but when a larger  $N$  value was used, especially values from EPA water quality standards, the system would become oversensitive and break. It would not model the growth accurately. In order to incorporate the EPA water quality standard values for  $N$ , the initial conditions needed to change where they followed the initial conditions set in [10]. Once this was done, the system responded with the realistic concentrations described in Figures 3.4, 3.5, and 3.6.

Lorenz describes this type of system sensitivity as the "butterfly effect" where a oversimplified system that is chaotic or near chaotic will be extremely sensitive to small changes to parameters or initial conditions and will cause a major change in the system. He experienced this with upper atmospheric weather modeling and his system of PDEs were simplified to a third order ODE.

Understanding parameter sensitivity occurs in systems describing natural systems is important so certain parameters do not reach unrealistic values such as what happened in 3.1, 3.2, and 3.3.

### **Observers Applied to Algae System**

Linear observer theory has been applied for parameter estimation in biological processes in depth for the understanding of algal growth systems. Nonlinear observer theory is still being explored. This thesis is one application of nonlinear observer theory by using a nonlinear sliding mode observer. This application shows potential for parameter estimation of nutrients for predicting algal blooms as well as observing growth for biological processes for biofuel.

## **4.1 Future Work**

### **4.1.1 Improve Model**

In order to improve the model the assumptions made beforehand need to be added back in: such as adding back light attenuation over water depth. The advection and diffusion terms can be added back and assume the algae is translating through the

water's surface in the  $x$  and  $z$  direction. As well as add in the hydrodynamic model described in [10] and couple with the algal growth system.

## 4.2 Implications of Research

Algae growth has caught a lot of attention due to recent blooms along the coast of California and Florida as well as its use for biofuel production. This section looks at how this thesis has the potential to be applied to these areas of research.

### Harmful Algal Bloom Modeling

Massive research efforts are focusing on methods to predict, prevent, and manage HABs. Any location with bodies of water can be subjected to these blooms and their negative impacts have both negative health and economic consequences. Empirical modeling efforts such as SPARROW can be used to help predict nutrient loads into water regions such as the Gulf Coast that are more susceptible to blooms as well as help prevent nutrient overload into sensitive bodies of water.

One method could be applying observers to a system based on a few measured inputs. This will allow researchers to estimate those parameters that are not easily measured and can help predict other parameters such as internal quotas and determine if a harmful bloom will occur or if the algal species is in equilibrium with its environment.

### Biofuel Development Modeling

Algae has been closely looked at for use as an alternative fuel source. There is a need for renewable carbon neutral biofuels that can replace petroleum-based fuels in order to mitigate greenhouse gases that are being released into the atmosphere. Microalgae are photosynthetic microorganisms that are capable of converting sunlight, water, carbon dioxide, and other nutrients into a biomass. That biomass produces oleaginous lipids that can be used in biofuel production [16].

Research in this area is already being conducted, and should continue to focus on optimizing the lipid production from algal biomass. Application of observer theory

can help estimate the amount of lipids that will be produced based on estimations of algal biomass concentrations as an example.

One effort focuses on utilizing readily available algae from present HABs. Scientists at Sandia National Labs are looking to harness the already deadly harmful algal blooms to create a renewable, domestic fuel source. Instead of establishing algae farms, this effort will focus on collecting the algae polluting California's coastal waters and converting this algae into biofuel[13].

Observer Theory is expanding into new areas of research that focus on biological processes. One major area is looking at state parameter estimation of algae biological processes in order to estimate parameters that are important for biofuel production. Parameters such as internal nitrogen quotas and lipid content are difficult to measure; but efforts from [7],[11],[12], [28], [29] and many more have the goal to apply state observers for parameter estimation in algal growth for biofuel production so we can be one step closer to removing our dependency on petroleum-based fuel in the future. This Master's Thesis looks to apply a nonlinear sliding mode observer to a simplified algal growth model in order to contribute to this active area of research.

# Appendix A

## Parameters Used for Algal Growth Simulation

Parameter	Value	Unit	Description
$\tilde{\mu}$	1.7	$day^{-1}$	growth rate
$Q_o$	0.050	$gN.gC^{-1}$	minimum internal nutrient quota required for growth
$Q_l$	0.25	$gN.gC^{-1}$	maximum achievable quota
$K_{iI}$	295	$\mu mol.m^{-2}s^{-1}$	derived constant
$K_{sI}$	70	$\mu mol.m^{-2}s^{-1}$	derived constant
$\bar{\lambda}$	0.073	$gN.gC^{-1}day^{-1}$	maximum uptake rate
$K_3$	0.0012	$gN.m^{-3}$	half saturation constant
$R$	0.0081	$day^{-1}$	biomass decay
$I_{o,max}$	500	$\mu mol.m^{-2}s^{-1}$	max incident light
$N$	0.17 $\rightarrow$ 1.7	$gN.m^{-3}$	controlled nitrate ( $NO_3$ ) input

Table A.1: Parameter values used for model

# Appendix B

## MATLAB Code

### Algae Model

- Equilibrium Points & Test Stability
- Nonlinear Model
- Plot

```
%Rebecca Griffith
```

```
%Algae Model Main Code
```

```
clear all
```

```
close all
```

```
% clc
```

```
tic
```

```
%SET PARAMETERS
```

```
global T K3 R Imax KsI KiI Qo Ql maxUR mu N dt u B
```

```
T = 10;           % [Days]           Time Observed
```

```
K3 = 0.0012;     % [gN/m3]       Half Saturation Rate
```

```
R = 0.0081;     % [1/day]           Mortality rate per day
```

```
Imax = 500;     % [umol/m2s] Light Intensity @ surface
```

```
KsI = 70;       % [umol/m2s] Derived constant
```

```
KiI = 295;     % [umol/m2s] Derived constant
```

```

Qo = 0.050;          % [gN/gC]      Minimum internal nutrient quota required for gro
Q1 = 0.25;          % [gN/gC]      Max achievable quota
maxUR = 0.073;     % [gN/gCday]    Max uptake rate (lambda bar)
mu = 1.7;          % [1/day]      Constant Derived
N = 1.2;           % [gN/m^3]     Constant Nutrient Input Rate:
dt = 0.0001;      % [s]          time step
u = N;             % [gN/m^3/day]  Control, the constant nutrient input rate
B = [0 0 1]';     %control (nutrient input)
de = 0.01;        % Deviation from Equiliberium
[Light] = LightModel(T,Imax); %LIGHT MODEL

```

## Equilibrium Points & Test Stability

```

gam = (mu*Imax)/(Imax + KsI + (Imax^2/KiI)); %easier to make a const. gamma in e
alpha = (Qo*gam)/(gam-R);
B = (R*alpha)/(1 - (alpha/Q1));
[x1star,x2star,x3star,A] = EquilibriumPoints(gam,alpha,B);
A;
eigenvalues = eig(A)
fprintf('x1star: %f \n',x1star);
fprintf('x2star: %f \n',x2star);
fprintf('x3star: %f \n',x3star);

```

```
eigenvalues =
```

```
1.0e+05 *
```

```
-1.3977
```

```
-0.0000
```

```
-0.0000
```

```

x1star: 2922.940630
x2star: 148.148148
x3star: 0.000009

```

## Nonlinear Model

### Initial Conditions

```

x1(1) = 20;      %gC/m^3  Biomass
x2(1) = 5;      %gN/m^3  Internal N
x3(1) = 5 + N;   %gN/m^3  External NO3
% x1(1) = x1star + de      %gC/m^3  Biomass
% x2(1) = x2star + de      %gN/m^3  Internal N
% x3(1) = x3star + de      %gN/m^3  External NO3
i = 0;
tnl = 0;
q(1) = x2(1)/x1(1);

```

```

for i=1:(T/dt)

```

```

    % NONLINEAR EQUATIONS WITH NO SMO AND LIGHT

```

```

    gam(i) = (mu*Light(i))/(Light(i) + KsI + (Light(i))^2/KiI); %easier to make a
    %time progression
    tnl(i+1)=tnl(i)+dt;

```

```

    %NO NEGATIVES

```

```

    if x1(i) < 0,
        x1(i) = 0;
    end
    if x2(i) < 0,
        x2(i) = 0;

```



```

end
if x3(i) < 0,
    x3(i) = 0;
end
q(i) = x2(i)/x1(i);    %internal nutrients per biomass unit

%    if q(i) = Inf,
%        q(i) = 0;
%    end
% Nitrate Uptake Rate Calculation (x)
lambda = maxUR*(x3(i)/(x3(i) + K3))*(1 - (q(i)/Q1));
%Macroalgae Growth Rate Calculation (x)
GrowthRate(i) = (gam(i)*(1-(Qo/q(i)))));

%Nonlinear Equations build F(x) WITH NO LIGHT
x1(i+1)=x1(i)+dt*(GrowthRate(i)*x1(i)-R*x1(i));
x2(i+1)=x2(i)+dt*(lambda*x1(i)-R*x2(i));
x3(i+1)=x3(i)+dt*(-(lambda*x1(i)) + N);
q(i+1) = q(i)+dt;
%NO NEGATIVES

end

```

## Plot

```

%BIOMASS
figure(1)
plot(tnl,x1)
xlabel('Day')
ylabel('Biomass(gC/m^3)')
title('Algae Biomass')

```

```

%NITROGEN
figure(2)
plot(tnl,x2)
xlabel('Day')
ylabel('Nitrogen (gN/m{3})')
title(' Internal Nitrogen')

%NUTRIENT
figure(3)
plot(tnl,x3)
xlabel('Day')
ylabel('Nutrients(gN/m{3})')
title('External Nitrate (NO{3})')

```

## Light

### light calculation

```

function [Light] = LightModel(T, dt, Imax);
global T K3 R Imax KsI KiI Qo Ql maxUR mu N dt u B
Imin = 0;
hr = linspace(0, 2*pi, (T/dt)*24);
Light = Imax*sin(T*hr);
Light(Light<0) = Imin;

end

```

## Linear State Observer

## Contents

- Equilibrium points

- Jacobian Matrix A

```
% Rebecca Griffith
```

```
%Equilibrium and Linearization with Jacobian A matrix
```

```
clear all
```

```
close all
```

```
clc
```

```
%Inputs
```

```
K3 = 0.0012;           % [gN/m^3]      Half Saturation Rate
```

```
R = 0.0081;           % [1/day]      Mortality rate per day
```

```
Imax = 500;           % [umol/m^2s] Light Intensity @ surface
```

```
KsI = 70;             % [umol/m^2s] Derived constant
```

```
KiI = 295;            % [umol/m^2s] Derived constant
```

```
Qo = 0.050;           % [gN/gC]      Minimum internal nutrient quota required for
```

```
Q1 = 0.25;            % [gN/gC]      Max achievable quota
```

```
maxUR = 0.073;        % [gN/gC/day]  Max uptake rate (lambda bar)
```

```
mu = 1.7;             % [1/day]      Constant Derived
```

```
N = 0.000009;        % [gN/m^3]      Constant Nutrient Input Rate
```

## Equilibrium points

```
%constants
```

```
gam = (mu*Imax)/(Imax + KsI + (Imax^2/KiI));
```

```
alpha = (Qo*gam)/(gam-R);
```

```
B = (R*alpha)/(1 - (alpha/Q1));
```

```
%equilibrium points
```

```
x3star = B*K3/(maxUR-B) %External Nitrates/Nutrients
```

```
beta = maxUR*(x3star/(x3star+K3)); %another constant
```

```
x1star = N/(beta*(1-(alpha/Q1))) % Biomass
```

```
x2star = alpha*x1star %Internal Nitrogen
```

```
x3star =
    8.5250e-06
```

```
x1star =
    0.0219
```

```
x2star =
    0.0011
```

## Jacobian Matrix A

```
%parts of matrix A: where A = [A11 A12 A13; A21 A22 A23; A31 A32 A33]
```

```
A11 = gam - ((2*Qo*x1star)/(x2star)) - R;
```

```
A21 = (maxUR*x3star)/(x3star+K3);
```

```
A31 = -(maxUR*x3star)/(x3star+K3);
```

```
A12 = -(((2*Qo*x1star*x2star) - Qo*x1star^2)/(x2star^2));
```

```
A22 = -((maxUR*x3star)/((x3star + K3)*Q1)) - R;
```

```
A32 = (maxUR*x3star)/((x3star + K3)*Q1);
```

```
A13 = 0;
```

```
A23 = (((maxUR*x1star)*(x3star+K3) - (maxUR*x1star*x3star))/((x3star+K3)^2)) - ...
      (((maxUR*x2star*Q1)*(x3star+K3) - (maxUR*x2star*x3star*Q1))/(((x3star+K3)*Q1)^2))
```

```
A33 = -(((maxUR*x1star)*(x3star+K3) - (maxUR*x1star*x3star))/((x3star+K3)^2)) + ...
      (((maxUR*x2star*Q1)*(x3star+K3) - (maxUR*x2star*x3star*Q1))/(((x3star+K3)*Q1)^2))
```

```
A = [A11 A12 A13; A21 A22 A23; A31 A32 A33]
```

```
[V, D] = eig(A)
```

```
T=10;
dt=0.0005;

t(1)=0;

e(:,1)=[1.1*x1star, 0.9*x2star, 1.1*x3star]';

C=[0 1 0];

P=[-2; -3; -4]';

L=(acker(A',C',P))'

L1 = [0.0692 0.0051 -0.0001]'

eh(:,1)=[0 0 0]';
ehh(:,1)=[0 0 0]';

k=1;
y(1)=0;

while t(k) < T,

    t(k+1)=t(k)+dt;

    e(:,k+1)=e(:,k)+dt*A*e(:,k);

    y(k+1)=C*e(:,k);
```

```

%linear observer

eh(:,k+1)=eh(:,k)+dt*(A*eh(:,k)+L*(y(k+1)-C*eh(:,k)));

%SM observer

ehh(:,k+1)=ehh(:,k)+dt*(A*ehh(:,k)+L1*sign(y(k+1)-C*ehh(:,k)));

k=k+1;

end

figure
plot(t,e(1,:)+x1star,'b',t,eh(1,:)+x1star,'k',t,ehh(1,:)+x1star,'m',t,t*0+x1star,'o')
%axis([0 T -0.02 0.06])
grid
legend('Location','best','Algal Biomass', 'linear observer estimate of biomass', 'SM observer estimate of biomass')
xlabel('Day')
ylabel('Algae Biomass (gC/m{3})')

figure
plot(t,e(2,:)+x2star,'b',t,eh(2,:)+x2star,'k',t,ehh(2,:)+x2star,'m',t,t*0+x2star,'o')
%axis([0 T -0.1 1])
grid
legend('Location','best','Internal Nitrogen', 'linear observer estimate of internal nitrogen', 'SM observer estimate of internal nitrogen')
xlabel('Day')
ylabel('Internal Nitrogen (gN/m{3})')

figure
plot(t,e(3,:)+x3star,'b',t,eh(3,:)+x3star,'k',t,ehh(3,:)+x3star,'m',t,t*0+x3star,'o')
%axis([0 10 0.00001 0.00002])
grid

```

```

legend('Location','best','External Nutrients', 'linear observer estimate of extern
xlabel('Day')
ylabel('External Nutrients in the form of NO_{3} (gN/m^{3})')

```

```

figure
subplot(3,1,1)
plot(t,e(1,:)+x1star,'r',t,t*0+x1star,'b')
axis([0 T 0.0 0.06])
xlabel('Day')
ylabel('Biomass(gC/m^3)');
legend('Location','best','With disturbance','At equilibrium')
title('System convergence towards equilibrium')
subplot(3,1,2)
plot(t,e(2,:)+x2star,'r',t,t*0+x2star,'b')
axis([0 T 0.9e-3 2.3e-3])
xlabel('Day')
ylabel('Internal Nitrogen(gN/m^3)')
legend('Location','best','With disturbance','At equilibrium')
subplot(3,1,3)
plot(t,e(3,:)+x3star,'r',t,t*0+x3star,'b')
axis([0 T -0.00001 0.00002])
xlabel('Day')
ylabel('External Nutrients(gN/m^3)')
legend('Location','best','With disturbance','At equilibrium')

```

A =

```

-1.3814    17.4904         0
 0.0005   -0.0102    1.0483
-0.0005    0.0021   -1.0483

```

V =

```
-1.0000    0.9996    0.9969
 0.0015    0.0204    0.0783
-0.0014   -0.0202   -0.0003
```

D =

```
-1.4068         0         0
         0   -1.0249         0
         0         0   -0.0081
```

L =

```
1.0e+03 *
-3.6681
 0.0066
 0.0100
```

L1 =

```
0.0692
 0.0051
-0.0001
```



**Equilibrium Points**

```
%Determine and test Equilibrium Points
```

```
function [x1star,x2star,x3star,A] = EquilibriumPoints(gam,alpha,B)
```

```
global T K3 R I KsI KiI Qo Ql maxUR mu N L dt u
```

```
%equilib consts.
```

```
x3star = B*K3/(maxUR-B);
```

```
beta = maxUR*(x3star/(x3star+K3));
```

```
x1star = N/(beta*(1-(alpha/Ql)));
```

```
x2star = alpha*x1star;
```

```
% Test Equilibrium Point
```

```
q = x2star/x1star; %internal nutrients per biomass unit
```

```
%Nitrate Uptake Rate Calculation
```

```
lambda = maxUR*(x3star/(x3star + K3))*(1 -(q/Ql));
```

```
%Macroalgae Growth Rate Calculation
```

```
GrowthRate = gam*(1-(Qo/q));
```

```
%Test equations: should be 0 as an output when equilibrium pts are plugged
```

```
%in
```

```
f1= GrowthRate*x1star- R*x1star;
```

```
f2= lambda*x1star - R*x2star;
```

```
f3= -lambda*x1star + N;
```

```
%Matrix A with Equilibrium pts plugged in: make matrix A easier to
```

```
%troubleshoot
```

```
%parts of matrix A: (row,column)
```

```
A11 = gam - ((2*Qo*x1star)/(x2star)) - R;
```

```
A21 = (maxUR*x3star)/(x3star+K3);
```

```
A31 = -(maxUR*x3star)/(x3star+K3);
```

```
A12 = -(((2*Qo*x1star*x2star) - Qo*x1star^2)/(x2star^2));
```

```

A22 = -((maxUR*x3star)/((x3star + K3)*Q1)) - R;
A32 = (maxUR*x3star)/((x3star + K3)*Q1);
A13 = 0;
A23 = (((maxUR*x1star)*(x3star+K3) - (maxUR*x1star*x3star))/((x3star+K3)^2)) - ...
      (((maxUR*x2star*Q1)*(x3star+K3) - (maxUR*x2star*x3star*Q1))/(((x3star+K3)*Q1)
A33 = -(((maxUR*x1star)*(x3star+K3) - (maxUR*x1star*x3star))/((x3star+K3)^2)) + ...
      (((maxUR*x2star*Q1)*(x3star+K3) - (maxUR*x2star*x3star*Q1))/(((x3star+K3)*Q1)^
A = [A11 A12 A13; A21 A22 A23; A31 A32 A33];
%eigenvalues of A. They should be less than 0 for stability
eval = eig(A);

```

## Nonlinear Sliding Mode Observer

### Contents

- Equilibrium Points & Test Stability
- SLIDING MODE OBSERVER

```

clear all
close all
% clc

%SET PARAMETERS
global T K3 R Imax KsI KiI Qo Q1 maxUR mu N L dt u B
T = 10;           % [Days]           Time Observed
K3 = 0.0012;      % [gN/m^3]           Half Saturation Rate
R = .0081;        % [1/day]            Mortality rate per day
Imax = 500;       % [umol/m^2s]        Light Intensity @ surface
KsI = 70;         % [umol/m^2s]        Derived constant
KiI = 295;        % [umol/m^2s]        Derived constant
Qo = 0.050;       % [gN/gC]            Minimum internal nutrient quota required for gro
Q1 = 0.25;        % [gN/gC]            Max achievable quota
maxUR = .073;     % [gN/gCday]         Max uptake rate (lambda bar)

```

```

mu = 1.7;           % [1/day]      Constant Derived
N = 0.000009;      % [gN/m^3/day]    Constant Nutrient Input Rate: DON'T
dt = 0.00001;      % [s]           time step
u = N;             % [gN/m^3/day]    Control, the constant nutrient input rate
B = [0 0 1]';      %control (nutrient input)

```

### Equilibrium Points & Test Stability

```

gam = (mu*Imax)/(Imax + KsI + (Imax^2/KiI)); %easier to make a const. gamma in e
alpha = (Qo*gam)/(gam-R);
B = (R*alpha)/(1 - (alpha/Q1))
[x1star,x2star,x3star,A] = EquilibriumPoints(gam,alpha,B);
A;
eigenvalues = eig(A)
fprintf('x1star: %f \n',x1star);
fprintf('x2star: %f \n',x2star);
fprintf('x3star: %f \n',x3star);

%When eigenvalues of A are negative the system is stable at the equilibrium
%points
%Equilibrium Points

B =

5.1494e-04

eigenvalues =

-1.4068
-1.0249

```

```
-0.0081
```

```
x1star: 0.021922
```

```
x2star: 0.001111
```

```
x3star: 0.000009
```

## SLIDING MODE OBSERVER

```
%ICs:
```

```
de = 0.00009*100;
```

```
%no deviation
```

```
xnl1(1) = x1star + de;
```

```
xnl2(1) = x2star +de;
```

```
xnl3(1) = x3star + de;
```

```
%with deviation
```

```
xnlh1(1) = x1star + de;
```

```
xnlh2(1) = x2star + de;
```

```
xnlh3(1) = x3star + de;
```

```
yh1(1)=0;
```

```
yh2(1)=0;
```

```
yh3(1)=0;
```

```
v1(1)=0;
```

```
v2(1)=0;
```

```
v3(1)=0;
```

```
v4(1)=0;
```

```
L1=0.01;
```

```
L2=1;
```

```
L3=10;
```

```

eps1=0.001;
eps2=0.00001;
eps3=0.1;

H1(1) = 0;
H2(1) = 0;
H3(1) = 0;

i = 0;
tnl = 0;
v(1)=0;
xdoth = [0; 0; 0];

% NONLINEAR EQUATIONS WITH SMO
gam = (mu*Imax)/(Imax + KsI + (Imax^2/KiI)); %easier to make a const. gamma in e
alpha = (Qo*gam)/(gam-R);
for i=1:(T/dt)
    %time progression
    tnl(i+1)=tnl(i)+dt;
    %for x
    q(i) = xnl2(i)/xnl1(i); %internal nutrients per biomass unit
    % Nitrate Uptake Rate Calculation (x)
    lambda = maxUR*(xnl3(i)/(xnl3(i) + K3))*(1 - (q(i)/Q1));
    %Macroalgae Growth Rate Calculation (x)
    GrowthRate = (gam*(1-(Qo/q(i)))));

    %Nonlinear Equations build F(x)
    xnl1(i+1)=xnl1(i)+dt*(GrowthRate*xnl1(i)-R*xnl1(i));
    xnl2(i+1)=xnl2(i)+dt*(lambda*xnl1(i)-R*xnl2(i));
    xnl3(i+1)=xnl3(i)+dt*(-(lambda*xnl1(i)) + N);

```

```
% SLIDING MODE OBSERVER
```

```
%BUILD H(x)
```

```
%Top row: H1 = y1
```

```
H1(i+1) = xn11(i)+dt*(xn12(i));
```

```
%Middle Row: H2 = y2
```

```
H2(i+1) = H2(i)+dt*((lambda*xn11(i)-R*xn12(i)));
```

```
%Bottom Row: H3 = y3
```

```
H3(i+1) = (((maxUR*xn13(i)/(xn13(i)+K3))*xn11(i))+ (((-maxUR*xn13(i)/(xn13(i)+K3))
            ((maxUR*(xn13(i)+K3)*xn11(i)-maxUR*xn11(i)*(xn13(i)^2))/((xn13(i)+K3)^2))
```

```
%Build V
```

```
v1(i+1) = xn12(i); %equivalent value 1
```

```
v2(i+1)=L1*sat((v1(i)-yh1(i))/eps1); %equivalent value 2
```

```
v3(i+1)=L2*sat((v2(i)-yh2(i))/eps2); %equivalent value 3
```

```
v4(i+1)=L3*sat((v3(i)-yh3(i))/eps3);
```

```
% Build Yh
```

```
yh1(i+1)=yh1(i)+dt*v2(i+1);
```

```
yh2(i+1)=yh2(i)+dt*v3(i+1);
```

```
yh3(i+1)=yh3(i)+dt*v4(i+1);
```

```
%sgnSigma=[sat((yh1(i)-H1(X))/eps, sat((yh2(i)-H2(X))/eps,sat((yh3(i)-H3(X))/ep
```

```
% L=L0*inv(dH/dx)
```

```
% L=L0*(dH/dx)'  
  
% XXh(i+1)=XXh(i)+dt*L*sgnSigma:  
  
V(:,i) = [v1(i); v2(i); v3(i)];  
  
%xdoth(:,i+1) = xdoth(:,i)+dt*(inv(dH(:,:,i))*[v2(i) v3(i) v4(i)]');  
end  
  
%Plot Nonlinear Model  
  
%MODEL WITH NO OBSERVER  
figure(1)  
plot(tnl,xnl1)  
xlabel('Day')  
ylabel('Biomass (gC/m{3})')  
title('Biomass Model')  
  
figure(2)  
plot(tnl,xnl2)  
xlabel('Day')  
ylabel('Nitrogen (gN/m{3})')  
title('Nitrogen Model')  
  
figure(3)  
plot(tnl,xnl3)  
xlabel('Day')  
ylabel('Nutrients (gN/m{3})')  
title('Nutrient Model')  
  
% SMO
```

```
figure(4)
plot(tn1,xn12,tn1,yh1)
xlabel('Day')
ylabel('Nitrogen(gN/m{3})')
legend('Nitrogen Model','Observer')
title('SMO')
```

```
%COMPARE H AND YH
figure(5)
plot(tn1,H1,tn1,yh1)
xlabel('time')
legend('y1','yh1')
title('y1 and yh1')
```

```
figure(6)
plot(tn1,H2,tn1,yh2)
xlabel('time')
legend('y2','yh2')
title('y2 and yh2')
```

```
figure(7)
plot(tn1,H3,tn1,yh3)
xlabel('time')
legend('y3','yh3')
title('y3 and yh3')
```



# Bibliography

- [1] Environmental Protection Agency. Mississippi river/gulf of mexico watershed nutrient task force: Report to congress. *EPA*, August 2017.
- [2] Environmental Protection Agency. Understanding gulf of mexico hypoxia using cmaq. *EPA*, June 2017.
- [3] Environmental Protection Agency. State progress toward developing numeric nutrient water quality criteria for nitrogen and phosphorus. *EPA*, May 2018.
- [4] Brian DO Anderson and John B Moore. *Optimal control: linear quadratic methods*. Courier Corporation, 2007.
- [5] Donald M Anderson. Approaches to monitoring, control and management of harmful algal blooms (habs). *Ocean & coastal management*, 52(7):342–347, 2009.
- [6] S Beale and B Shafai. Robust control system design with a proportional integral observer. *International Journal of Control*, 50(1):97–111, 1989.
- [7] Micaela Benavides, Daniel Coutinho, Anne-Lise Hantson, Jan Van Impe, and Alain Vande Wouwer. Robust luenberger observers for microalgal cultures. *Journal of Process Control*, 36:55–63, 2015.
- [8] Birgitta Bergman, Gustaf Sandh, Senjie Lin, John Larsson, and Edward J Carpenter. Trichodesmium—a widespread marine cyanobacterium with unusual nitrogen fixation properties. *FEMS Microbiology reviews*, 37(3):286–302, 2013.

- [9] Olivier Bernard. Hurdles and challenges for modelling and control of microalgae for co2 mitigation and biofuel production. *Journal of Process Control*, 21(10):1378–1389, 2011.
- [10] Olivier Bernard, Anne-Céline Boulanger, Marie-Odile Bristeau, and Jacques Sainte-Marie. A 2d model for hydrodynamics and biology coupling applied to algae growth simulations. *ESAIM: Mathematical Modelling and Numerical Analysis*, 47(5):1387–1412, 2013.
- [11] Olivier Bernard and J-L Gouzé. State estimation for bioprocesses. Technical report, 2002.
- [12] Olivier Bernard, Gauthier Sallet, and Antoine Sciandra. Nonlinear observers for a class of biological systems: application to validation of a phytoplanktonic growth model. *IEEE Transactions on Automatic Control*, 43(8):1056–1065, 1998.
- [13] Jules Bernstein. The good, the bad and the algae. *Sandia National Labs: News: Sandia assists NASA with several shuttle projects*, Aug 2017.
- [14] Fred Brauer, Carlos Castillo-Chavez, and Carlos Castillo-Chavez. *Mathematical models in population biology and epidemiology*, volume 40. Springer, 2012.
- [15] David E Burmaster. The unsteady continuous culture of phosphate-limited *monochrysis lutheri* droop: experimental and theoretical analysis. *Journal of experimental marine Biology and Ecology*, 39(2):167–186, 1979.
- [16] Yusuf Chisti. Biodiesel from microalgae beats bioethanol. *Trends in biotechnology*, 26(3):126–131, 2008.
- [17] R DeCarlo, S Zak, and S Drakunov. Variable structure and sliding mode control. chapter in the control handbook a volume in the electrical engineering handbook series, 1996.
- [18] Sergey Drakunov and Vadim Utkin. Sliding mode observers. tutorial. In *Decision and Control, 1995., Proceedings of the 34th IEEE Conference on*, volume 4, pages 3376–3378. IEEE, 1995.

- [19] Sergey V Drakunov. Sliding-mode observers based on equivalent control method. In *Decision and Control, 1992., Proceedings of the 31st IEEE Conference on*, pages 2368–2369. IEEE, 1992.
- [20] Sergey V Drakunov and Victor J Law. Parameter estimation using sliding mode observers: application to the monod kinetic model. *Chemical Product and Process Modeling*, 2(3):21, 2007.
- [21] Sergey V Drakunov and Vadim I Utkin. Sliding mode control in dynamic systems. *International Journal of Control*, 55(4):1029–1037, 1992.
- [22] SV Drakunov. An adaptive quasioptimal filter with discontinuous parameters. *Automatika i Telemekhanika*, (9):76–86, 1983.
- [23] Michaël R Droop. 25 years of algal growth kinetics a personal view. *Botanica marina*, 26(3):99–112, 1983.
- [24] Christopher Edwards, Sarah K Spurgeon, and Ron J Patton. Sliding mode observers for fault detection and isolation. *Automatica*, 36(4):541–553, 2000.
- [25] Aleksej Fedorovič Filippov. *Differential equations with discontinuous righthand sides: control systems*, volume 18. Springer Science & Business Media, 2013.
- [26] Karen F Gaines, Dwayne E Porter, Susan A Dyer, Gary R Wein, John E Pinder, and I Lehr Brisbin. Using wildlife as receptor species: a landscape approach to ecological risk assessment. *Environmental management*, 34(4):528–545, 2004.
- [27] Patricia M Glibert, J Icarus Allen, AF Bouwman, Christopher W Brown, Kevin J Flynn, Alan J Lewitus, and Christopher J Madden. Modeling of habs and eutrophication: status, advances, challenges. *Journal of marine systems*, 83(3-4):262–275, 2010.
- [28] Guillaume Goffaux, Alain Vande Wouwer, and O Bernard. Continuous-discrete interval observers for monitoring microalgae cultures. *Biotechnology progress*, 25(3):667–675, 2009.

- [29] Jean-Luc Gouzé, Alain Rapaport, and Mohamed Zakaria Hadj-Sadok. Interval observers for uncertain biological systems. *Ecological modelling*, 133(1-2):45–56, 2000.
- [30] RD Hill, RG Rinker, and H Dale Wilson. Atmospheric nitrogen fixation by lightning. *Journal of the Atmospheric Sciences*, 37(1):179–192, 1980.
- [31] Anne B Hoos and Gerard McMahon. Spatial analysis of instream nitrogen loads and factors controlling nitrogen delivery to streams in the southeastern united states using spatially referenced regression on watershed attributes (sparrow) and regional classification frameworks. *Hydrological Processes: An International Journal*, 23(16):2275–2294, 2009.
- [32] Thomas Kailath. *Linear systems*, volume 156. Prentice-Hall Englewood Cliffs, NJ, 1980.
- [33] Niloofar N. Kamran. *Sliding Mode Observers for Distributed Parameter Systems: Theory and Applications*. PhD thesis, 2016. Copyright - Database copyright ProQuest LLC; ProQuest does not claim copyright in the individual underlying works; Last updated - 2017-03-14.
- [34] D Karl, A Michaels, B Bergman, D Capone, El Carpenter, R Letelier, F Lipschultz, H Paerl, D Sigman, and L Stal. Dinitrogen fixation in the world's oceans. In *The Nitrogen Cycle at Regional to Global Scales*, pages 47–98. Springer, 2002.
- [35] Samuel Kitchen-McKinley. *Nonlinear observers for human-in-the-loop control systems*. PhD thesis, 2010. Copyright - Database copyright ProQuest LLC; ProQuest does not claim copyright in the individual underlying works; Last updated - 2016-03-10.
- [36] Dirk P Kroese, Tim Brereton, Thomas Taimre, and Zdravko I Botev. Why the monte carlo method is so important today. *Wiley Interdisciplinary Reviews: Computational Statistics*, 6(6):386–392, 2014.

- [37] David Luenberger. Observers for multivariable systems. *IEEE Transactions on Automatic Control*, 11(2):190–197, 1966.
- [38] Francis Mairet, Olivier Bernard, Thomas Lacour, and Antoine Sciandra. Modelling microalgae growth in nitrogen limited photobioreactor for estimating biomass, carbohydrate and neutral lipid productivities. *IFAC Proceedings Volumes*, 44(1):10591–10596, 2011.
- [39] Peter S Maybeck. *Stochastic models, estimation, and control*, volume 3. Academic press, 1982.
- [40] FB Metting. Biodiversity and application of microalgae, 1996.
- [41] Jacques Monod. The growth of bacterial cultures. *Annual Reviews in Microbiology*, 3(1):371–394, 1949.
- [42] US Department of Commerce, National Oceanic, and Atmospheric Administration. Harmful algal blooms, Nov 2009.
- [43] University of Hawaii: College of Education. Exploring our fluid earth, 2018.
- [44] JCH Peeters and P Eilers. The relationship between light intensity and photosynthesis: a simple mathematical model. *Hydrobiological Bulletin*, 12(2):134–136, 1978.
- [45] GE Schwarz, AB Hoos, RB Alexander, and RA Smith. The sparrow surface water-quality model: theory, application and user documentation. *US geological survey techniques and methods report, book*, 6(10):248, 2006.
- [46] SP Seitzinger, JA Harrison, Egon Dumont, Arthur HW Beusen, and AF Bouwman. Sources and delivery of carbon, nitrogen, and phosphorus to the coastal zone: An overview of global nutrient export from watersheds (news) models and their application. *Global Biogeochemical Cycles*, 19(4), 2005.
- [47] Karl Sigmund. Kolmogorov and population dynamics. pages 177–186, 2007.
- [48] National Geographic Society. Mapping u.s. watersheds, Aug 2015.

- [49] V Utkin. Sliding modes in control and optimization, ser. communications and control engineering series, 1992.
- [50] Ivayla Vatcheva, Hidde De Jong, Olivier Bernard, and Nicolaas JI Mars. Experiment selection for the discrimination of semi-quantitative models of dynamical systems. *Artificial Intelligence*, 170(4-5):472–506, 2006.
- [51] Casey Watson, Sean Bailey, Jamie Arnold, Brad Dickerson, Nia Watson, Audrey Biesk, and Samantha Kummerer. Everything you need to know about the florida red tide, Aug 2018.
- [52] Bong Wie. *Space Vehicle Dynamics and Control 2nd Edition*. American Institute of Aeronautics and Astronautics, 2006.